

การหาสัมประสิทธิ์การถ่ายโอนมวลระหว่างก๊าซคาร์บอนไดออกไซด์กับสารละลายมอนอเอทานอลเอมีน 2-เมทิลอะมิโนเอทานอล และไดเมทิลอะมิโนเอทานอลในหอดูดซึมแบบแผ่น



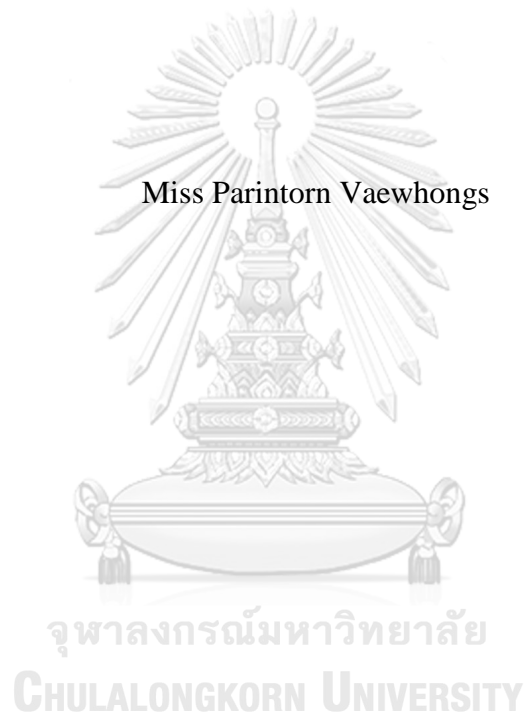
บทคัดย่อและแฟ้มข้อมูลฉบับเต็มของวิทยานิพนธ์ตั้งแต่ปีการศึกษา 2554 ที่ให้บริการในคลังปัญญาจุฬาฯ (CUIR) เป็นแฟ้มข้อมูลของนิสิตเจ้าของวิทยานิพนธ์ ที่ส่งผ่านทางบัณฑิตวิทยาลัย

The abstract and full text of theses from the academic year 2011 in Chulalongkorn University Intellectual Repository (CUIR) are the thesis authors' files submitted through the University Graduate School.

วิทยานิพนธ์นี้เป็นส่วนหนึ่งของการศึกษาตามหลักสูตรปริญญาวิศวกรรมศาสตรมหาบัณฑิต
สาขาวิชาวิศวกรรมเคมี ภาควิชาวิศวกรรมเคมี
คณะวิศวกรรมศาสตร์ จุฬาลงกรณ์มหาวิทยาลัย
ปีการศึกษา 2560
ลิขสิทธิ์ของจุฬาลงกรณ์มหาวิทยาลัย

DETERMINATION OF MASS TRANSFER COEFFICIENT OF CO₂ IN SOLUTIONS OF MONOETHANOLAMINE, 2-(METHYLAMINO)ETHANOL AND DIMETHYLAMINOETHANOL IN PACKED ABSORPTION COLUMN

Miss Parintorn Vaewhongs



A Thesis Submitted in Partial Fulfillment of the Requirements
for the Degree of Master of Engineering Program in Chemical Engineering
Department of Chemical Engineering
Faculty of Engineering
Chulalongkorn University
Academic Year 2017
Copyright of Chulalongkorn University

Thesis Title DETERMINATION OF MASS TRANSFER
COEFFICIENT OF CO₂ IN SOLUTIONS OF
MONOETHANOLAMINE, 2-
(METHYLAMINO)ETHANOL AND
DIMETHYLAMINOETHANOL IN PACKED
ABSORPTION COLUMN

By Miss Parintorn Vaewhongs

Field of Study Chemical Engineering

Thesis Advisor Associate Professor Tawatchai Charinpanitkul,
D.Eng.

Thesis Co-Advisor Assistant Professor Kreangkrai Maneeintr, Ph.D.

Accepted by the Faculty of Engineering, Chulalongkorn University in
Partial Fulfillment of the Requirements for the Master's Degree

..... Dean of the Faculty of Engineering
(Associate Professor Supot Teachavorasinskun, D.Eng.)

THESIS COMMITTEE

..... Chairman
(Professor Suttichai Assabumrungrat, Ph.D.)

..... Thesis Advisor
(Associate Professor Tawatchai Charinpanitkul, D.Eng.)

..... Thesis Co-Advisor
(Assistant Professor Kreangkrai Maneeintr, Ph.D.)

..... Examiner
(Chalida Klaysom, Ph.D.)

..... External Examiner
(Winyu Tanthapanichakoon)

ปริบทรววหงษ์ : การหาสัมประสิทธิ์การถ่ายโอนมวลระหว่างก๊าซคาร์บอนไดออกไซด์กับสารละลายมอนอเอทานอลเอมีน 2-เมทิลอะมิโนเอทานอล และไดเมทิลอะมิโนเอทานอลในหอดูดซึมแบบแพ็ค (DETERMINATION OF MASS TRANSFER COEFFICIENT OF CO₂ IN SOLUTIONS OF MONOETHANOLAMINE, 2-(METHYLAMINO)ETHANOL AND DIMETHYLAMINOETHANOL IN PACKED ABSORPTION COLUMN) อ.ที่ปรึกษาวิทยานิพนธ์หลัก: รศ.ชวรัชชัชชินพาศิษกุล, อ.ที่ปรึกษาวิทยานิพนธ์ร่วม: ผศ.เกรียงไกร มณีอินทร์, 84 หน้า.

วิทยานิพนธ์ฉบับนี้ ได้ศึกษาปัจจัยต่างๆที่มีผลต่อการถ่ายโอนมวลสารของสารใหม่ 2 ชนิด ได้แก่ 2-เอทิลอะมิโนเอทานอล และไดเมทิลอะมิโนเอทานอล เปรียบเทียบกับมอนอเอทานอลเอมีน จากการศึกษาอิทธิพลของชนิดสาร อิทธิพลปริมาณคาร์บอนไดออกไซด์ขาเข้าในสารดูดซึมที่ 0.0 0.1 และ 0.2 โมลต่อโมล อิทธิพลความเข้มข้นสารดูดซึมที่ 3 4 และ 5 กิโลโมลต่อลูกบาศก์เมตร อิทธิพลอัตราการไหลของสารดูดซึมที่ 5.3 10.6 และ 15.9 ลูกบาศก์เมตรต่อตารางเมตรต่อชั่วโมง และอิทธิพลปริมาณคาร์บอนไดออกไซด์ในสถานะที่ร้อยละ 13 14 และ 15 โดยปริมาตร พบว่า 2-เมทิลอะมิโนเอทานอลให้อัตราการถ่ายโอนมวลสารสูงที่สุด โดยสูงที่สุดที่ 1.2656 กิโลโมลต่อกิโลปาสกาลต่อชั่วโมงต่อลูกบาศก์เมตร คาร์บอนไดออกไซด์ขาเข้าในสารดูดซึมที่ 0.0 โมลต่อโมล สารดูดซึมเข้มข้นที่ 3 กิโลโมลต่อลูกบาศก์เมตร อัตราการไหลสารดูดซึมที่ 10.6 ลูกบาศก์เมตรต่อตารางเมตรต่อชั่วโมง และปริมาณคาร์บอนไดออกไซด์ในก๊าซที่ร้อยละ 15 โดยปริมาตร ซึ่งสูงกว่ามอนอเอทานอลเอมีน และไดเมทิลอะมิโนเอทานอลที่สถานะเดียวกันที่ 0.4638 และ 0.0215 กิโลโมลต่อกิโลปาสกาลต่อชั่วโมงต่อลูกบาศก์เมตร ตามลำดับ ปัจจัยที่มีผลต่ออัตราการถ่ายโอนมวลสารที่สุดคือความเข้มข้นของสารตั้งต้นซึ่งช่วยเสริมอัตราการเกิดปฏิกิริยาไปข้างหน้าและช่วยลดเวลาในการเกิดปฏิกิริยาดูดซึมคาร์บอนไดออกไซด์ที่ละลายลงในเอมีน ดังนั้น เมื่อตัววัดสมรรถนะ (enhancement factor) มีค่าเพิ่มขึ้นจึงส่งผลให้สัมประสิทธิ์การถ่ายโอนมวลโดยรวมเพิ่มขึ้นด้วย ในการศึกษาครั้งนี้ ไดเมทิลอะมิโนเอทานอลซึ่งเป็นเอมีนตติยภูมิไม่สามารถดูดซึมก๊าซคาร์บอนไดออกไซด์ได้หมดในทุกการทดลอง อันเนื่องมาจากอัตราการเกิดปฏิกิริยาที่ช้าเนื่องจากขั้นตอนการเกิดกรดคาร์บอนิก ถึงแม้ว่ายังมีปัจจัยอีกมากมายที่ต้องทำการศึกษาก่อนนำสารดูดซึมไปใช้ในอุตสาหกรรมการกำจัดคาร์บอนไดออกไซด์จริง 2-เมทิลอะมิโนเอทานอลได้แสดงให้เห็นถึงความเป็นไปได้ที่จะเป็นสารดูดซึมที่ดี

ภาควิชา	วิศวกรรมเคมี	ลายมือชื่อ นิสิต
สาขาวิชา	วิศวกรรมเคมี	ลายมือชื่อ อ.ที่ปรึกษาหลัก
ปีการศึกษา	2560	ลายมือชื่อ อ.ที่ปรึกษาร่วม

5870189621 : MAJOR CHEMICAL ENGINEERING

KEYWORDS: OVERALL MASS TRANSFER COEFFICIENT / 2-(METHYLAMINO)ETHANOL / DIMETHYLAMINOETHANOL / PACKED ABSORPTION COLUMN / CO₂ CHEMISORPTION

PARINTORN VAEWHONGS: DETERMINATION OF MASS TRANSFER COEFFICIENT OF CO₂ IN SOLUTIONS OF MONOETHANOLAMINE, 2-(METHYLAMINO)ETHANOL AND DIMETHYLAMINOETHANOL IN PACKED ABSORPTION COLUMN. ADVISOR: ASSOC. PROF.TAWATCHAI CHARINPANITKUL, D.Eng., CO-ADVISOR: ASST. PROF.KREANGKRAI MANEEINTR, Ph.D., 84 pp.

In this study, mass transfer of two new solvents, 2-MAE and DMAE were studied with various factors affecting mass transfer coefficient in comparison with MEA. Effect of solvent types, CO₂ inlet loading 0.0, 0.1 and 0.2 mol/mol, solvent concentration 3, 4 and 5 kmol/m³, solvent flow rate 5.3, 10.6 and 15.9 m³/(m²·h) and CO₂ content 13-15 v/v% in gas feed were investigated. In all cases, 2-MAE performed highest mass transfer rate among others. The highest mass transfer rate was 1.2656 kmol/(kPa·h·m³) for the case that CO₂ inlet loading 0.0 mol/mol, solvent concentration 3 kmol/m³, solvent flow rate 10.6 m³/(m²·h) and CO₂ content in gas feed was 15 v/v% which higher than that of MEA and DMAE at 0.4638 and 0.0215, respectively. The most influencing factor on rate of mass transfer was the reactant concentration which promoted forward rate of reaction and consequently reduced time required for absorption of dissolved CO₂. Therefore, an increase in enhancement factor leads to an increase in overall mass transfer coefficient. In this study, DMAE which is a tertiary amine was not able to reach 100% CO₂ removal efficiency due to the sluggish rate of reaction in carbonic formation step. Though there are more subjects needed to be investigated before further implementation in real CO₂ capture plants, 2-MAE showed a positive possibility to be a candidate for solvent selection.

Department: Chemical Engineering Student's Signature

Field of Study: Chemical Engineering Advisor's Signature

Academic Year: 2017 Co-Advisor's Signature

ACKNOWLEDGEMENTS

I would like give my gratitude to my thesis advisor Assoc. Prof. Dr. Tawatchai Charinpanitkul and also to my thesis co-advisor Asst. Prof. Dr. Kreangkrai Maneeintr for giving me my encouragement to pursue this dissertation till the end and also academic knowledge. My grateful appreciation also to Prof. Dr. Suttichai Assabumrungrat as a chairman, Dr. Chalida Klaysom and Dr. Winyu Tanthapanichakoon as an external examiner for their advice and comments.

This work would not be accomplished without financial support from Center of Excellence in Particle Technology (CEPT) and Ratchadapisek Sompoch Endowment Fund (2016) (CU-059-003-IC), Chulalongkorn University.

Sincere thanks to my colleagues in CEPT and especially TRG members for your helpfulness. You always have my back.

Last but not least, my full-hearted thanks to my parents for their unconditional love and great support, my lovely friends at ChE23 KU and SHC25 and she who has given me understanding and love through the years.

CONTENTS

	Page
THAI ABSTRACT	iv
ENGLISH ABSTRACT.....	v
ACKNOWLEDGEMENTS.....	vi
CONTENTS.....	vii
List of Figures	ix
List of Tables	xi
CHAPTER 1 INTRODUCTION.....	1
1.1 Background and motivation.....	1
1.2 Sources of CO ₂ emission	2
1.3 Types of CO ₂ combustion process.....	4
1.3.1 Post Combustion Process.....	4
1.3.2 Oxyfuel Combustion Process.....	4
1.3.3 Pre Combustion Process.....	5
1.4 CO ₂ capture technologies for post combustion process	5
1.4.1 Absorption.....	5
1.4.2 Adsorption.....	6
1.4.3 Membrane technology.....	7
1.5 Objective.....	8
1.6 Scope.....	8
CHAPTER 2 THEORIES AND LITERATURE REVIEW.....	10
2.1 Chemical absorption process	10
2.2 Absorbent selection for chemical absorption.....	11
2.3 Criteria of absorbent selection	13
2.4 Mass transfer in absorption column.....	19
2.4.1 Calculation of overall mass transfer coefficient.....	23
2.4.2 Literature Review	27
CHAPTER 3 EXPERIMENT.....	30
3.1 Chemicals	30

	Page
3.2 Experimental method.....	30
3.2.1 Packed column operation	30
3.2.2 Solvent concentration and CO ₂ loading calculation.....	32
3.3 Scope of experiment	34
CHAPTER 4 RESULTS AND DISCUSSION.....	35
4.1 Reaction regime	35
4.2 Effect of solvent types	38
4.3 Effect of CO ₂ inlet loading	44
4.4 Effect of solvent concentration.....	53
4.5 Effect of solvent flow rate	57
4.6 Effect of inert gas flow rate	62
CHAPTER 5 CONCLUSION.....	70
5.1 Conclusion	70
5.2 Recommendation	72
REFERENCES	74
APPENDIX.....	77
VITA.....	84

List of Figures

Figure 1.1 World composition of GHGs in 2010	2
Figure 1.2 CO ₂ emitted from assorted world economic sectors in 2010	3
Figure 1.3 CO ₂ emission by sector in Thailand, 2014	3
Figure 2.1 Chemical absorption process	11
Figure 2.2 Gas liquid interface.....	19
Figure 2.3 Packed column with CO ₂ mole balance on elemental section	23
Figure 3.1 Experimental setup	32
Figure 3.2 CO ₂ loading analyzer	33
Figure 4.1 CO ₂ reaction in liquid film for fast reaction regime.....	38
Figure 4.2 Overall mass transfer coefficient of MEA, 2-MAE and DMAE.....	39
Figure 4.3 Reaction pathway of primary, secondary and tertiary amines	40
Figure 4.4 CO ₂ outlet loading of MEA, 2-MAE and DMAE	40
Figure 4.5 CO ₂ concentration in bulk gas of MEA, 2-MAE and DMAE against height.....	43
Figure 4.6 Overall mass transfer coefficient of MEA, 2-MAE and DMAE.....	44
Figure 4.7 CO ₂ outlet loading of MEA, 2-MAE and DMAE	48
Figure 4.8 CO ₂ concentration in bulk gas of MEA against height	49
Figure 4.9 CO ₂ concentration in bulk gas of 2-MAE against height	49
Figure 4.10 CO ₂ concentration in bulk gas of DMAE against height	50
Figure 4.11 Overall mass transfer coefficient of MEA, 2-MAE and DMAE.....	53
Figure 4.12 CO ₂ outlet loading of MEA, 2-MAE and DMAE	55
Figure 4.13 CO ₂ concentration in bulk gas of MEA against height	55
Figure 4.14 CO ₂ concentration in bulk gas of 2-MAE against height.....	56
Figure 4.15 CO ₂ concentration in bulk gas of DMAE against height	56
Figure 4.16 Overall mass transfer coefficient of MEA, 2-MAE and DMAE.....	58
Figure 4.17 CO ₂ outlet loading of MEA, 2-MAE and DMAE	60
Figure 4.18 CO ₂ concentration in bulk gas of MEA against height	60

Figure 4.19 CO ₂ concentration in bulk gas of 2-MAE against height	61
Figure 4.20 CO ₂ concentration in bulk gas of DMAE against height	61
Figure 4.21 Overall mass transfer coefficient of MEA, 2-MAE and DMAE.....	63
Figure 4.22 CO ₂ outlet loading of MEA, 2-MAE and DMAE	66
Figure 4.23 CO ₂ concentration in bulk gas of MEA against height	67
Figure 4.24 CO ₂ concentration in bulk gas of 2-MAE against height	67
Figure 4.25 CO ₂ concentration in bulk gas of DMAE against height	68



List of Tables

Table 2.1 Basic properties of MEA, 2-MAE and DMAE.....	12
Table 2.2 Characteristics of each absorbent	18
Table 2.3 Mass transfer characteristic of amine absorbents in packed column.....	28
Table 3.1 Scope of investigation.....	34
Table 4.1 pK_a value of solvents	42
Table 4.2 $K_G a_v$ of solvents at each CO_2 inlet loading capacity.....	45
Table 4.3 Titration of MEA, 2-MAE and DMAE before and after the experiment.....	47
Table 4.4 $K_G a_v$ of solvents at each solvent at 3, 4 and 5 $kmol/m^3$	54
Table 4.5 $K_G a_v$ of solvents at each solvent flow rate	59
Table 4.6 Henry's constant at 298 K	64

CHAPTER 1

INTRODUCTION

1.1 Background and motivation

Green House Gases (GHGs) are gas molecules that absorb and emit the heat radiation partly deliver to the outer space and partly remain on the surface of the earth. According to Figure 1.1, the main composition of GHGs is carbon dioxide (CO₂) which is up to 76% [1] of GHGs. This phenomenon is called Greenhouse Effect. In the past, greenhouse gases had maintained the warm temperature of the earth in order to create a suitable atmosphere for living things. However, a drastic increase in amount of CO₂ after industrial revolution from 280 ppm to 400 ppm [2] has led to global warming which causes various negative impacts such as a rise in temperature, ozone depletion, ocean acidification and so on. These impacts do not only harm life on earth, but also are prone to be worse due to growing concentration of CO₂ each year. In 2014, International Panel on Climate Change (IPCC) predicted that the CO₂ concentration will reach 500-1000 ppm by the end of 2100 [1]. Therefore, mitigation of GHGs emission, especially CO₂, must be applied.

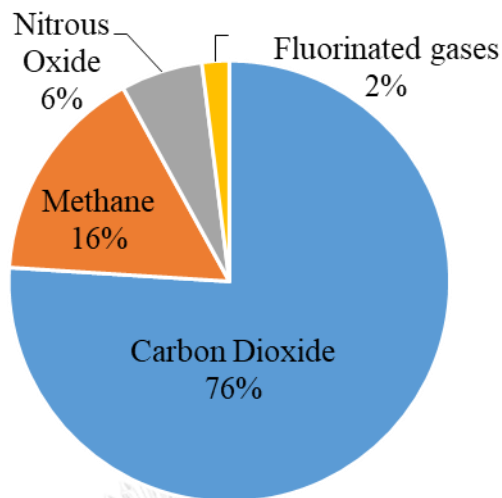


Figure 1.1 World composition of GHGs in 2010

1.2 Sources of CO₂ emission

CO₂ was released from many sources as shown in Figure 1.2. Approximately 70% of CO₂ was released from three sectors: Electricity and heat production, industry and agriculture, forestry and other land use [1]. Noticed that, one fourth of CO₂ is released from power generation sector, where reducing emission of CO₂ from power generation sector would be a promising way to reduce CO₂ emission. Despite nearly the equivalent amount of CO₂ emitted from each of that sector, CO₂ capture from agriculture, forest and other land use sector is barely viable due to scattering locations of emission, uncontrollable concentration of emitted CO₂ and non-cost effective process.

In Thailand, Figure 1.3 shows that up to 40% of CO₂ emission was released from power generation sector [3]. According to world's and Thailand's statistic, power generation is a major source of CO₂ emission. Thus, development of CO₂ capture

process in order to reduce CO₂ from power generation would be an effective method to reduce CO₂ emission.

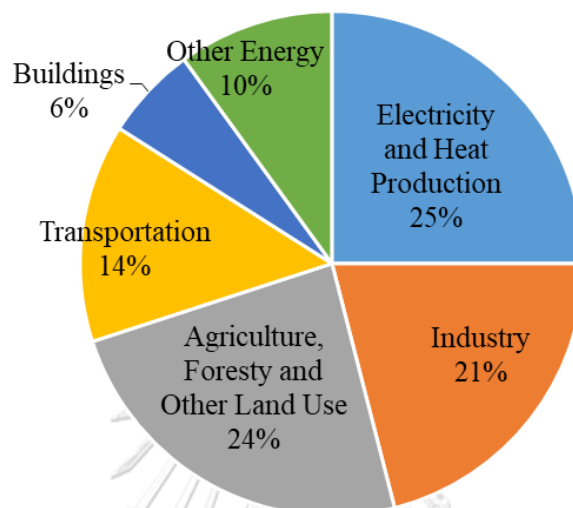


Figure 1.2 CO₂ emitted from assorted world economic sectors in 2010

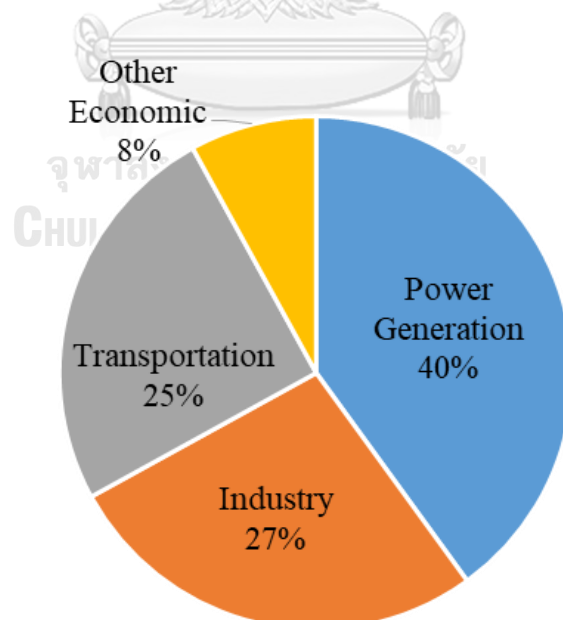


Figure 1.3 CO₂ emission by sector in Thailand, 2014

1.3 Types of CO₂ combustion process

The different sources of CO₂ emission yield distinct ranges of CO₂ concentration so that they require particular capture techniques. Three processes classified by the concentration of emitted CO₂ are described below.

1.3.1 Post Combustion Process

This process captures CO₂ from the normal combustion process between carbonaceous fuel and excess air to produce steam for power generation. The steam is supplied to a turbine in order to produce electricity. CO₂-containing stream is separated by chemical absorption or other appropriate capture methods to extract CO₂. At least 38 percent of CO₂ from energy and heat production sector is released by post combustion process [1].

The concentration of CO₂ from the combustion process is relatively low i.e. 12-18 v/v% for coal-fired power plants [4] and approximately only 4-8 v/v% for gas-fired power plants [4]. Besides, some industries such as cement kilns, refining plants, steel plants, etc, are fitted into this category. Capture of CO₂ from this process can also be retrofitted to the existing plant sites.

1.3.2 Oxyfuel Combustion Process

The oxyfuel combustion process is similar to post combustion process except that pure or almost pure oxygen is used instead of air. Prior to being fed to the combustion zone, N₂ is separated from the stream therefore the concentration of CO₂ in the product stream is higher than 80 v/v% [5]. This process consumes large amount of air in order to provide enough pure amount of O₂ which mostly supplied by air separation unit. Nevertheless, capture of CO₂ from oxy fuel combustion process is

relatively new to industry, there are only few demonstration plants being constructed [6].

1.3.3 Pre Combustion Process

CO₂ from this process occurs from the reaction between syngas and steam (water-gas shift reaction) called gasification. H₂ produced from this process creates electricity and could be used in fuel cell for transportation in the future. Syngas is a product of combustion reaction between fuel and pure oxygen. As a result, the approximate CO₂ concentration is 25-40 v/v% and pressure is in the range of 2.5-5 MPa [5]. Compared with post combustion process, both oxyfuel and pre combustion processes give high concentration of CO₂ so CO₂ from the latter processes could be easier to separate.

1.4 CO₂ capture technologies for post combustion process

At present, there are three main technologies for capture CO₂ in post combustion process. Each technology has its own advantages and disadvantages as described below.

1.4.1 Absorption

Absorption is a process that a molecule or atom of substance uptakes another into itself. There are two types of absorption processes; one is chemical absorption and the other is physical absorption.

In chemical absorption, gas stream flows in a countercurrent pattern with liquid. The concentration of CO₂ in the gas stream depends on the types of combustion

processes CO₂ released. The liquid stream is an absorbent stream which is mostly amine solution. Monoethanolamine (MEA) is a commercial absorbent that is widely used due to its high efficiency of CO₂ absorption and fast absorption rate. However, the disadvantages of MEA are low CO₂ loading capacity, high energy consumption for absorbent regeneration, equipment corrosion, and amine degradation [5], [7]. Li X et al. reported that 80 percent of energy consumed is for regeneration of absorbent [8]. The solution to this problem is to develop a new absorbent that could compensate MEA's downside and also gives adequate efficiency for CO₂ absorption.

On the other hand, physical absorption of CO₂ is based on Henry's law. According to the principle, CO₂ would be absorbed at low temperature and high pressure and vice versa - desorbed at low pressure and high temperature [5]. Chakravati et al. reported that this process is not economical with CO₂ lower than 15 v/v% in flue gas streams [9]. Thus, physical absorption is rather suitable for the process with high CO₂ vapor pressure; in other words this process is not appropriate with CO₂ capture in post combustion process which is the main focus of this study.

1.4.2 Adsorption

To capture CO₂ with this technique, CO₂ is fed through packed solid adsorbents in a reactor. Typical adsorbents are zeolites, activated carbon, alumina or even amine-based solid [8]. After fully adsorbed, the regeneration process takes place usually by heating or reducing pressure which refers to temperature swing adsorption (TSA) and pressure swing adsorption (PSA), respectively. Adsorption process consumes lower energy compare with chemical absorption. The major drawback of this process is low CO₂ selectivity of adsorbents, especially with low CO₂ partial pressure in flue gas

stream from power plants in post-combustion process [8, 10]. To capture CO₂ from post combustion process, adsorbents need to be developed to gain high percentage of CO₂ selectivity.

1.4.3 Membrane technology

In membrane technology, CO₂ capture techniques are classified into two main types of membrane systems (1) Gas separation membrane of which film makes itself a barrier between two streams and allows only CO₂ to pass through the other side of selective membrane and high purity CO₂ stream is further captured by another CO₂ capture unit. The driving force is a difference in pressure between two sides of membrane. Thus, high pressure is applied in this technique. (2) Gas absorption membrane where gas stream and liquid solvent flow in a countercurrent pattern on each side of membrane. CO₂ from gas side flows across through selective membrane and then chemically absorbed by liquid solvent, usually MEA. Compared with chemical absorption in packed column, these allow membrane separation techniques to have compact size and avoid channeling and entrainment [10]. However, limitation of this technique is separation efficiency which depends on partial pressure of CO₂ in flue gas stream. Thus, it is more suitable for CO₂ partial pressure higher than 20 v/v% [10].

Among the three methods mentioned above, chemical absorption is the most promising CO₂ capture technology for post combustion process due to its high capture efficiency and retrofitting to existing power plants which are the main focus of this work [2]. Physical absorption, adsorption and membrane separation are less compatible with chemical absorption because of low efficiency at low partial pressure of CO₂.

However, the disadvantages of chemical absorption with MEA as liquid absorbent are high energy consumption and equipment corrosion. To improve these problems, new liquid absorbents must be developed.

In this study, Monoethanolamine (MEA), 2-(Methylamino)ethanol (2-MAE) and Dimethylaminoethanol (DMAE) were selected as liquid absorbents as a result of their potential in CO₂ loading capacity and their properties as primary, secondary and tertiary amines in CO₂ absorption. Mass transfer coefficient is a significant factor to design an absorption column so this study emphasizes on determining mass transfer coefficient of 2-MAE and DMAE, comparing with commercial MEA.

1.5 Objective

To determine overall mass transfer coefficient of 2-MAE and DMAE in packed column under ambient temperature and pressure and compare their efficiency with commercial alkanolamine, MEA.

1.6 Scope

- 1.6.1 Type of solvents MEA, 2-MAE and DMAE
- 1.6.2 Solvent flow rate 5.3, 10.6 and 15.9 m³/(m²·h)
- 1.6.3 CO₂ concentration 13.0, 14.0 and 15.0 v/v%
- 1.6.4 Inlet CO₂ loading 0.0, 0.1, 0.2 mol/mol
- 1.6.5 Solvent concentration at 3, 4 and 5 kmol/m³

CO₂ and N₂ concentration are between 13.0-15.0 v/v% which falls in CO₂ concentration region from post combustion process. Total gas flow rate was fixed at 4 L/min. Ambient temperature and pressure are used.



CHAPTER 2

THEORIES AND LITERATURE REVIEW

2.1 Chemical absorption process

As shown in Figure 2.1, the typical absorption process starts from feeding simulated flue gas of CO₂, along with N₂, at the bottom of the absorption unit. Absorbent flows down from the top, then gas and liquid stream come into contact with each other in a countercurrent pattern. As a result of mass transfer, CO₂ dissolves into liquid and absorption consequently takes place. Other gases flow out of the column. After CO₂ is absorbed, CO₂ rich solvent flows into heat exchanger to exchange heat between rich solvent and lean solvent streams in order to reduce heat consumption in reboiler which aims to increase the temperature of rich solvent stream from normally 40°C in absorption unit to around 120-150°C in desorption unit [10]. In desorption unit, CO₂ rich solvent flows downward from the top of desorption unit, while CO₂-absorbent bond is destroyed by heat and gaseous CO₂ moves upward and further compressed for transportation or usage. On the other hand, lean solvent stream passes through heat exchanger and is subsequently cooled to around 40°C.

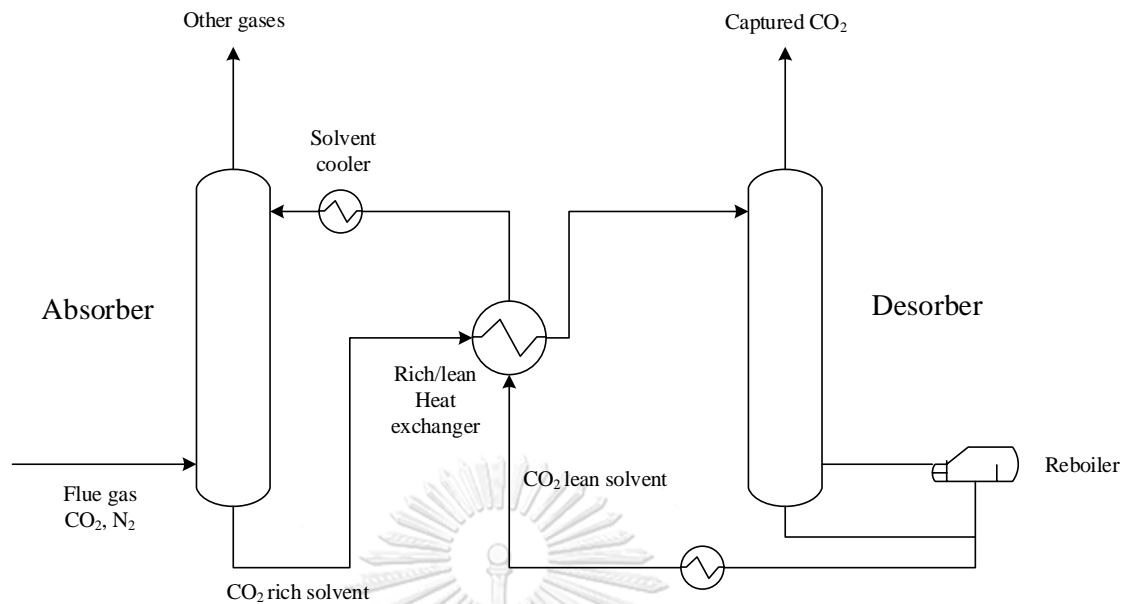


Figure 2.1 Chemical absorption process


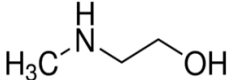
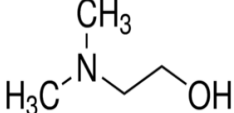
One of the factor that directly affects CO₂ absorption efficiency is absorbent. Consequently, absorbent selection is the primary key to gain high efficiency of CO₂ capture process.

2.2 Absorbent selection for chemical absorption

Alkanolamines have been widely used in industries in order to capture CO₂ from flue gas. Alkanolamines are compounds which consist of hydroxyl (-OH) and amino (-NH₂, -NH and -NR₂) groups. Amines are structurally classified into three groups which each has its own specific properties: primary (-NH₂), secondary (-NH) and tertiary (-NR₂) amines. In this work, MEA, 2-MAE and DMAE are studied to determine overall mass transfer coefficient. RNH₂ were often used as a representative of all types of amines, which were MEA, 2-MAE and DMAE, in this dissertation.

Before choosing any absorbents one should know basic properties of each absorbent as shown in Table 2.1.

Table 2.1 Basic properties of MEA, 2-MAE and DMAE

Absorbents	Structures	Type	Molecular Weight (g/mol)	Density, 20°C (g/cm ³)
Monoethanolamine (MEA)		Primary	61.08	1.02
2-(Methylamino)ethanol (2-MAE)		Secondary	75.11	0.94
(Dimethylamino)ethanol (DMAE)		Tertiary	89.14	0.89

MEA has long been used as CO₂ absorbent in industrial scale, because, as roughly described in previous chapter, fast reaction rate, more than 90 percent CO₂ capture efficiency [2] and high mass transfer coefficient due to its uncomplicated primary amine structure. Moreover, low molecular weight of MEA compared to other amines leads to higher amine concentration at the same amount of weight. However, its major disadvantage is high energy consumption, nearly up to 80 percent of overall energy consumed. Not only MEA requires energy-intensive process, but also it can degrade into nitrosamines and nitramines [11].

2.3 Criteria of absorbent selection

To choose an amine to be a potential candidate for CO₂ absorbent in commercial scale, there are many properties that should be considered such as solubility, kinetics, heat regeneration cost, physical properties, mass transfer, etc. Some major effects that impact CO₂ absorption efficiency would be described below.

Solubility of CO₂ in liquid absorbent is usually the first parameter many researchers decide to study. The study involves with thermodynamics which is vapor-liquid equilibrium (VLE) of CO₂ and liquid absorbent at various temperatures and CO₂ partial pressures. VLE can determine the maximum mol of CO₂ absorbed per mole of absorbent, which is called *CO₂ loading capacity*, abbreviated as α . High CO₂ loading capacity means less amount of solvents is required to capture equivalent CO₂ content in gas stream. Another important parameter that could be achieved from study VLE behavior of the system is *Cyclic capacity*. Cyclic capacity is the difference of CO₂ loading capacity at absorption and desorption temperature, which normally operates at 40°C and 150°C and 8 bar [12], respectively. High cyclic capacity solvent leads to more CO₂ that could be absorbed in absorption unit and less solvent circulation rate. Therefore, in industrial applications, an absorbent that occupies high CO₂ but low cyclic capacity might not be economically interesting.

Kinetics data is essential in order to determine reaction mechanism, order of reaction and rate constant of each reaction. Reaction mechanism between CO₂ and alkanolamine depends on structure and basicity of alkanolamines [13]. The mechanism

between aqueous solution of primary, secondary and tertiary amines and CO₂ can be explained by the following set of equations [14]

Carbamate formation



Protonation of alkanolamine



Hydrolysis and ionization of dissolved CO₂



Ionization of water



For primary and secondary amines, the mechanism occurs as in Equation (2.1) through Equation (2.4). Firstly, alkanolamine (RNH₂) reacts with CO₂ forming carbamate ion (RNHCOO⁻) and proton(H⁺). Alkanolamine also simultaneously reacts with proton to produce alkanolammonium (RNH₃⁺). Reaction between CO₂ and H₂O is relatively slow compare to that of Equation (2.1) and Equation (2.2). The proton produced from carbamate formation and protonation of alkanolamine would be used up to yield alkanolamine as in Equation (2.2). Therefore, primary amines normally achieve maximum 0.5 mol/mol of CO₂ loading capacity whereas secondary amines, of which carbamate formation is not as dominant, would result in higher CO₂ loading capacity

than primary amines (but less than 1.0 mol/mol). Equation (2.1) through (2.4) could be used for secondary amines with a change of amine formula from RNH_2 to RNH . Summing up Equation (2.1) and Equation (2.2), Zwitterion Mechanism [15] is obtained below



On the other hand, tertiary amines exhibit lower reaction rate because carbamate cannot be produced by Equation (2.1) according to their chemical structure (R_3N). As a result, CO_2 does not directly react with tertiary amines so Equation (2.1) does not occur in this case. In case of tertiary amines, CO_2 is literally absorbed by water, not amines. However, Equation (2.3) and (2.4) are still valid, but Equation (2.2) must be rewritten to match with their structure.

Protonation of alkanolamine (tertiary amines)



Reaction between tertiary amines and CO_2 resulting from combining Equation (2.3) together with (2.6) are called Based-Catalyzed Hydration [15] as shown in Equation (2.7). Stoichiometric ratio of amine to CO_2 is 1:1 so that tertiary amines possess higher CO_2 loading than primary and secondary amines.



Despite higher CO₂ loading capacity, tertiary amines display slower rate of absorption compare to primary and secondary amines. This is due to the fact that rate of absorption of CO₂ into water is inferior to amines [14].

Mass transfer coefficient between CO₂ and absorbent is required in order to theoretically estimate absorption column height which affects both fixed and operating cost in industrial plants. At the same operating condition, each individual absorbent has its own mass transfer characteristic depending on its structure and pKa value [13]. For each absorbent, various factors affecting mass transfer coefficient are absorbent flow rate, inert gas flow rate (CO₂ concentration in gas phase), absorbent concentration and CO₂ inlet loading in absorbent [16-19]. Here, each factor would be briefly described why they need to be investigated. The study of effect of solvent types would be to find a new solvent that could substitute the commercial one such as MEA in order to compensate the disadvantages as suggested in Chapter 1 and also exhibit a comparative CO₂ capture efficiency. In this work, mass transfer characteristics of MEA (commercial), 2-MAE and DMAE would be examined. Dependence of CO₂ concentration in bulk gas would be analyzed to observe the change in mass transfer coefficient and CO₂ capture efficiency because, in industrial plants, CO₂ inlet flue gas could not be controlled constant all the time [5]. Therefore, the study of CO₂ concentration around 13-15 v/v% (still in range of post combustion process) is an important task. Absorbent concentration is another important parameter that would be studied. Clearly, an increase in solvent concentration would lead to an increase in absorbed molecules of CO₂. However, economic balances would be taken into account in term of CO₂ loading capacity. In regeneration process, it is impossible to desorb all

CO₂ chemically and physically bonding with amines. Also, as stated in *Solubility*, an essential parameter is cyclic capacity of interested amines; thus, determination of mass transfer at different CO₂ inlet loading is necessary.

In this study, the mentioned parameters that influence mass transfer characteristics would be experimentally investigated. Derivation of mass transfer coefficient and concept would be thoroughly discussed in the next section.

Heat of regeneration is an important parameter that leads to energy consumption and consequently consumes upto 70-80% in total process cost [2]. Energy consumed by regeneration of MEA is upto 3.3 GJ/tCO₂ [20]. Therefore, an attempt to find a new solvent which contributes to lower heat of regeneration in order to reduce total process cost becomes an essential task.

Physical properties of solvents extensively studied are density, viscosity and physical N₂O solubility. Excluding mass transfer coefficient, density and viscosity at different temperatures and flow rates are important to determine the dimension of absorption unit due to circulation of absorbent. When CO₂ dissolves in alkanolamines, reaction also takes place so N₂O, which is analogous to CO₂ in structure and molecular weight, is physically absorbed in aqueous solution without chemical reaction. Thus, N₂O is used to measure Henry's constant instead of CO₂ itself [21]. Data can be further used in VLE modelling.

Corrosion is another factor needed to be considered when observing for long-term use. For economic purpose, a raise in solvent concentration from 2.5 to 3.5

kmol/m³ led to more CO₂ removal efficiency per mole of solvent and also fixed cost and operating cost per year was relatively lower from 1.0 and 1.0 to 0.56 and 0.33, respectively [22]. Though there are some studies of corrosion inhibitor at present to break through the limitations, however, too high solvent concentration would result in some equipment corrosion problems. Selection of solvents to use in acid gas treating process, corrosion is another important topic to be considered.

Table 2.2 Characteristics of each absorbent

Absorbent Characteristics	MEA	2-MAE	DMAE	Reference
Solubility (40°C, 3 kmol/m ³), mol/mol	0.523	0.556	0.639	[23, 24]
Mass transfer rate, kmol/(kPa·h·m ³)	0.29	-	-	[16]
Rate constant, m ³ /(kmol·s)	2,187.3	-	-	[15]
Heat of Regeneration, GJ/tCO ₂	3.3	-	-	[20]
Price, THB/dm ³	237	1,500	562	*

*Based on price at time of purchased from Ligand Scientific Co. Ltd. (MEA) on 8/8/2016 and Scientific Promotion Co. Ltd. (2-MAE and DMAE) 12/9/2017

Apart from these aforementioned properties, there are other properties that would also be taken into account to study alkanolamines in other viewpoints, for instance chemical stability and biodegradability. However, this research will focus on the determination of overall mass transfer coefficient and its dependence on studied factors.

2.4 Mass transfer in absorption column

Mass transfer is the key phenomenon in absorption process. Mass transfer occurs between bulk gas and liquid phases when they come into contact on the surface of packing. Gas liquid interface is illustrated in Figure 2.2.

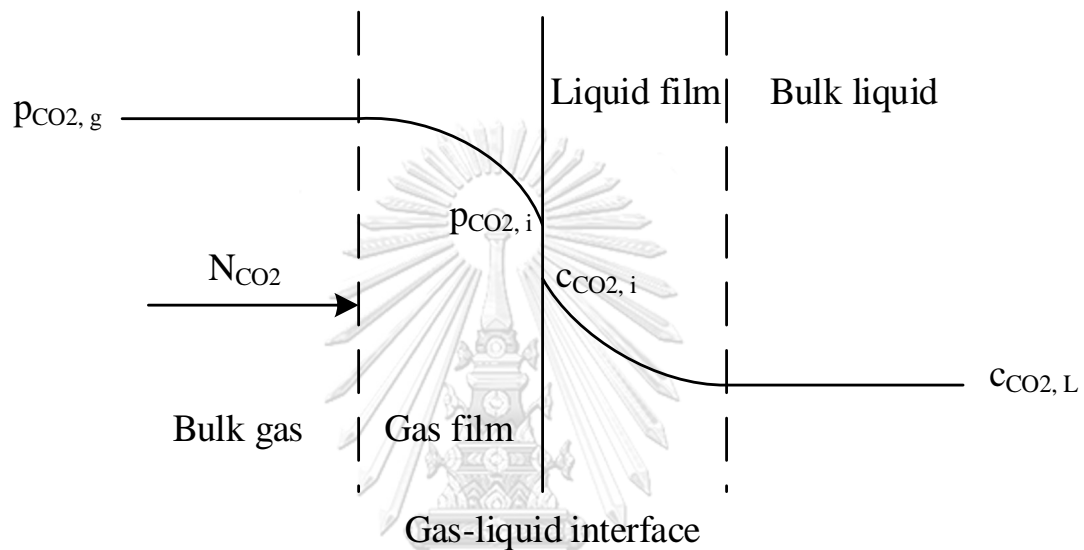


Figure 2.2 Gas liquid interface

This phenomenon can be explained by Two Film Theory proposed by Whitman [25]. CO_2 in bulk gas phase which the partial pressure ($p_{\text{CO}_2, g}$) represented the concentration in gas phase diffuses to gas-liquid interface due to concentration gradient through gas film. The convective mass transfer coefficient in gas phase is denoted as k_G . At gas-liquid interface, the equilibrium is reached. Liquid-equilibrium concentration of gas at interface is defined as $c_{\text{CO}_2, i}$. Equilibrium relationship between $p_{\text{CO}_2, i}$ and $c_{\text{CO}_2, i}$ can be calculated by Henry's Law as shown in Equation (2.8) where H is Henry's constant.

$$p_{\text{CO}_2,i} = Hc_{\text{CO}_2,i} \quad (2.7)$$

CO₂ dissolves into liquid phase and diffuses through liquid film which its mass transfer coefficient in liquid phase is designated as k_L^0 . After passing through liquid film, CO₂ diffuses into bulk liquid phase. The driving force of the system is concentration gradient.

Gas and liquid rate of diffusion can be written as Equation (2.9) and Equation (2.10) as follows

$$N_{\text{CO}_2} = k_G(p_{\text{CO}_2,g} - p_{\text{CO}_2,i}) \quad (2.8)$$

$$N_{\text{CO}_2} = k_L^0(c_{\text{CO}_2,i} - c_{\text{CO}_2,L}) \quad (2.9)$$

However, it is difficult to mathematically determine each mass transfer coefficient because there are no equipment that could directly measure partial pressure or concentration at gas-liquid interface. Thus, overall mass transfer coefficient is employed. Based on gas phase, the overall mass transfer coefficient is symbolized as K_G . Then, overall mass transfer flux between gas and liquid bulk can be expressed as Equation (2.10).

$$N_{\text{CO}_2} = K_G(p_{\text{CO}_2,g} - p_{\text{CO}_2}^*) \quad (2.10)$$

where $p_{\text{CO}_2}^*$ is an equilibrium vapor pressure of $c_{\text{CO}_2,L}$ relating by Henry's law as in Equation (2.8). Substitute Henry's law in Equation (2.10) gives

$$N_{\text{CO}_2} = K_G(p_{\text{CO}_2,g} - Hc_{\text{CO}_2,L})$$

Moreover, overall gas and liquid mass transfer coefficient gas can be expressed in term of resistance by deriving Equation (2.10) with the aid of Henry's law.

$$\frac{1}{K_G} = \frac{p_{\text{CO}_2,g} - p_{\text{CO}_2}^*}{N_{\text{CO}_2}}$$

$$\frac{1}{K_G} = \frac{p_{\text{CO}_2,g} - p_{\text{CO}_2,i}}{N_{\text{CO}_2}} + \frac{p_{\text{CO}_2,i} - p_{\text{CO}_2}^*}{N_{\text{CO}_2}}$$

$$\frac{1}{K_G} = \frac{p_{\text{CO}_2,g} - p_{\text{CO}_2,i}}{N_{\text{CO}_2}} + \frac{H(c_{\text{CO}_2,i} - c_{\text{CO}_2,L})}{N_{\text{CO}_2}}$$

From the set of equations above, two forms of total resistance of the system are written as Equation (2.11) and Equation (2.12).

$$\frac{1}{K_G} = \frac{1}{k_G} + \frac{H}{k_L} \quad (2.11)$$

$$\frac{1}{K_L} = \frac{1}{hk_G} + \frac{1}{k_L} \quad (2.12)$$

However, in case of mass transfer with chemical reaction taking place as CO_2 absorption into amines, CO_2 transfer in liquid film would be different from non-reaction

phenomena. Chemical reaction in liquid film maintains high driving force in liquid film [22]. When CO₂ dissolves in amines, chemical reaction occurs so that concentration of CO₂ in bulk liquid is kept low. Meanwhile for non-chemical reaction, CO₂ concentration in liquid phase increases as more CO₂ molecules are absorbed along the length of the column. Therefore, rate of mass transfer with chemical reaction is higher than rate of mass transfer with absence of chemical reaction [22]. At this point, enhancement factor is introduced as fluxes of CO₂ with chemical reaction to fluxes of CO₂ without chemical reaction as in Equation (2.13)

$$I = \frac{k_L(c_{\text{CO}_2,i} - c_{\text{CO}_2,L})}{k_L^0(c_{\text{CO}_2,i} - c_{\text{CO}_2,L})} = \frac{k_L}{k_L^0} \quad (2.13)$$

If I=1, there is no chemical reaction takes place in liquid film so mass transfer coefficient in two cases are equal. If I>1, there is chemical reaction occurs in liquid film and the reaction promotes mass transfer in liquid film [22]. With simultaneous chemical reaction and mass transfer, overall mass transfer coefficient based on gas phase as in Equation (2.11) and (2.12) could be rewritten as in Equation (2.14) and (2.15) below:

$$\frac{1}{K_G} = \frac{1}{k_G} + \frac{H}{Ik_L} \quad (2.14)$$

$$\frac{1}{K_L} = \frac{1}{hk_G} + \frac{1}{Ik_L} \quad (2.15)$$

According to Equation (2.14) and (2.15), if I>1, chemical reaction promotes mass transfer in liquid film and also enhances overall mass transfer coefficient.

2.4.1 Calculation of overall mass transfer coefficient

To calculate overall mass transfer coefficient, it is normally based on unit volume of absorption tower rather than interfacial area between gas and liquid phase or wetted surface area in packed column. In order to achieve this, Equation (2.10) is multiplied both sides by a_v , to express fluxes of CO_2 and overall mass transfer coefficient based on unit volume of absorber as in Equation (2.16).

$$N_{\text{CO}_2} a_v = K_G a_v P (y_{\text{CO}_2, \text{g}} - y_{\text{CO}_2}^*) \quad (2.16)$$

However, the term $N_{\text{CO}_2} a_v$ could not be experimentally determined so, in order to determine $K_G a_v$, we need to substitute $N_{\text{CO}_2} a_v$ term to a calculable one. When a closer look is taken to an elemental section of packed tower as illustrated in Figure 2.3, one could derive a mole balance on CO_2 as shown below.

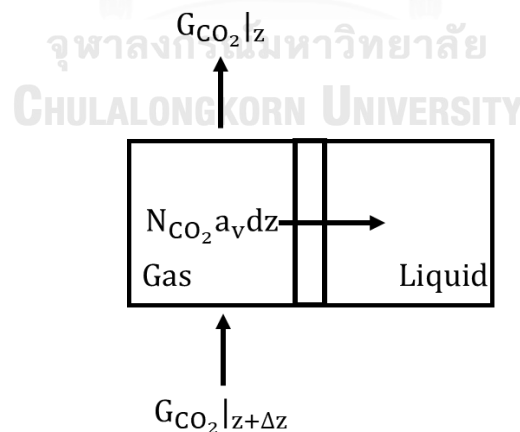


Figure 2.3 Packed column with CO_2 mole balance on elemental section

For steady state operation, total molar flow rate of CO_2 into an elemental section must be equal with total molar flow rate of CO_2 outlet from that section. At any height

Z , molar flow rate of CO_2 (G_{CO_2}) in terms of inert gas flow rate and concentration of CO_2 in bulk gas could be written as Equation (2.17)

$$G_{\text{CO}_2}|_z = G_I \left(\frac{y_{\text{CO}_2,g}}{y_{\text{N}_2,g}} \right) |_z = G_I \left(\frac{y_{\text{CO}_2,g}}{1-y_{\text{CO}_2,g}} \right)_z \quad (2.17)$$

According to mole balance principle, $K_G a_v$ could be determined as stated below

$$G_{\text{CO}_2}|_{z+\Delta z} = N_{\text{CO}_2} a_v dz + G_{\text{CO}_2}|_z$$

Substitution of Equation (2.17) would yield

$$\begin{aligned} G_I \left(\frac{y_{\text{CO}_2,g}}{1-y_{\text{CO}_2,g}} \right)_{z+\Delta z} &= N_{\text{CO}_2} a_v dz + G_I \left(\frac{y_{\text{CO}_2,g}}{1-y_{\text{CO}_2,g}} \right)_z \\ N_{\text{CO}_2} a_v &= G_I \left(\frac{y_{\text{CO}_2,g}}{1-y_{\text{CO}_2,g}} \right)_{z+\Delta z} - G_I \left(\frac{y_{\text{CO}_2,g}}{1-y_{\text{CO}_2,g}} \right)_z \\ N_{\text{CO}_2} a_v &= G_I \frac{d \left(\frac{y_{\text{CO}_2,g}}{1-y_{\text{CO}_2,g}} \right)}{dz} \end{aligned} \quad (2.18)$$

where Y is a mole ratio of CO_2 to N_2 and could be expressed mathematically as

$$Y = \frac{y_{\text{CO}_2,g}}{y_{\text{N}_2,g}} = \frac{y_{\text{CO}_2,g}}{1-y_{\text{CO}_2,g}}. \text{ Thus, Equation (2.18) could be written in term of } Y \text{ instead of}$$

$y_{\text{CO}_2,g}$.

$$N_{\text{CO}_2} a_v = G_I \frac{dY}{dz} \quad (2.19)$$

Substitute $N_{\text{CO}_2} a_v$ from Equation (2.19) into Equation (2.16) would yield

$$G_I dY = K_G a_v P (y_{\text{CO}_2, g} - y_{\text{CO}_2}^*) dz$$

$$dz = \frac{G_I dY}{K_G a_v P (y_{\text{CO}_2, g} - y_{\text{CO}_2}^*)}$$

According to the study of Zeng et al, the reaction between amines and CO_2 could assume to be very fast leading to zero concentration of CO_2 in liquid phase ($x_{\text{CO}_2} = 0$) [26]. Therefore, $y_{\text{CO}_2}^*$ which is an equilibrium concentration of CO_2 in bulk gas is subsequently zero. Also, $y_{\text{CO}_2, g}$ could be written in term of mole ratio as $y_{\text{CO}_2, g} = \frac{Y}{1+Y}$. Then, we would get dz in term of Y .

$$dz = \frac{G_I}{K_G a_v P} \left(\frac{1+Y}{Y} \right) dY$$

Integration from top to bottom of the column would yield

$$\int_{z=0}^{z=H} dz = \frac{G_I}{K_G a_v P} \int_{Y=Y_{z=0}}^{Y=Y_{z=H}} \left(\frac{1+Y}{Y} \right) dY = \frac{G_I}{K_G a_v P} \int_{Y=Y_{z=0}}^{Y=Y_{z=H}} \left(\frac{1}{Y} + Y \right) dY$$

$$H = \frac{G_I}{K_G a_v P} (\ln Y + Y) \Big|_{Y_{z=0}}^{Y_{z=H}}$$

$$H = \frac{G_I}{K_G a_v P} [(\ln Y_{z=H} + Y_{z=H}) - (\ln Y_{z=0} + Y_{z=0})]$$

$$H = \frac{G_I}{K_G a_v P} \left[\left(\ln \frac{Y_{z=H}}{Y_{z=0}} \right) + (Y_{z=H} - Y_{z=0}) \right]$$

$K_G a_v$ could be experimentally determined from Equation (2.20) by sampling CO_2 concentration at top and bottom of the column.

$$K_G a_v = \frac{G_I}{HP} \left[\ln \frac{Y_{z=H}}{Y_{z=0}} + (Y_{z=H} - Y_{z=0}) \right] \quad (2.20)$$

As Equation (2.20), $K_G a_v$ could be evaluated by known parameters with the unit of $\text{kmol}/(\text{m}^3 \cdot \text{kPa} \cdot \text{h})$. G_I is inert gas flow rate which is, in this case, N_2 flow rate ($\text{kmol}/\text{m}^2 \cdot \text{h}$), H is height from bottom of the column that CO_2 concentration in bulk gas has been taken to measure and P is total pressure of the system which is, in this case, at atmospheric pressure of 101.325 kPa. The evaluation of $K_G a_v$ with this method is successfully reported by many researchers [26].

In case of random packed column system, $K_G a_v$ is considered constant throughout the column. There are three factors contributing to a change in $K_G a_v$ which are (I) interfacial area between gas and liquid phase (or in this study, wetted surface area of packing) (II) resistance in gas side and (III) resistance in liquid side. As of (I), solvent flow rate is constant throughout an experiment, thus wetted surface area between gas and liquid remains constant. (II) 85% of inlet gas composed of N_2 which remains constant throughout the column, so little effect of gas flow rate is found on $K_G a_v$. (III) Resistance in liquid side is constant in an experiment so the thickness of liquid film is consistent and unchanged [18, 19, 26].

To evaluate CO₂ capture efficiency of each experiment, CO₂ removal efficiency could be simply determined from the difference of inlet and outlet CO₂ volumetric percentage in gas phase as in Equation (2.21)

$$\text{CO}_2 \text{ removal efficiency (\%)} = \frac{\text{CO}_{2,\text{inlet}} - \text{CO}_{2,\text{outlet}}}{\text{CO}_{2,\text{inlet}}} \times 100 \quad (2.21)$$

2.4.2 Literature Review

In this work, 2-MAE and DMAE were chosen to study their mass transfer coefficient in packed column because of their higher solubility than MEA. For 2-MAE aqueous solution, Haider et al. [24] reported that at 313K and solvent concentration of 1.0M comparing with MEA, 2-MAE performed higher CO₂ loading capacity at every partial pressure of CO₂ loading, due to unstable carbamate formation. 2-MAE also performed higher solubility, when compared with other amines such as Diethanolamine (DEA) and 2-amino-2-methyl-1,3-propanediol (AMPD) which are secondary and sterically hindered amines, respectively. Reaction mechanism between secondary amine and CO₂ can be described by Zwitterion Mechanism [15].

Aruno et al. [23] studied solubility of 3.0M DMAE, as a tertiary amine, at 313K and range of CO₂ partial pressure of 5-100 kPa, exhibited higher CO₂ loading compared with 3.0M MEA and Methyldiethanolamine (MDEA), another commercialized amine. Tertiary amine usually performs higher CO₂ loading which could be explained by Base-Catalyzed Hydration Mechanism [15].

Literature review on mass transfer characteristic is summarized in Table 2.3. Effect of structured and dumped packing were studied by Aroonwilas et al. [16]. The result showed that structured packing gave better mass transfer characteristic because

of high surface area to volume ratio, uniform liquid distribution and lower pressure drop. However, channeling and high cost were major disadvantages of structured packing so, in this study, dumped packing would be used.

Table 2.3 Mass transfer characteristic of amine absorbents in packed column

Absorbent	Types of packing	Column Diameter (mm)	Concentration (kmol/m ³)	Liquid flow rate (mL/min)	Reference
AMP	Sulzer-EX	19	2	24-71	[16]
DEAB	Sulzer-DX	30.3	1-3	40-90	[17]
DEAB	Sulzer-DX	275	2	3960-6930	[19]
MDEA-MEA	Sulzer-EX	275	2.3/0.5-1.95/1.16	2772-4950	[27]
1DMA2P	Random	28	1-3	27-77	[18]

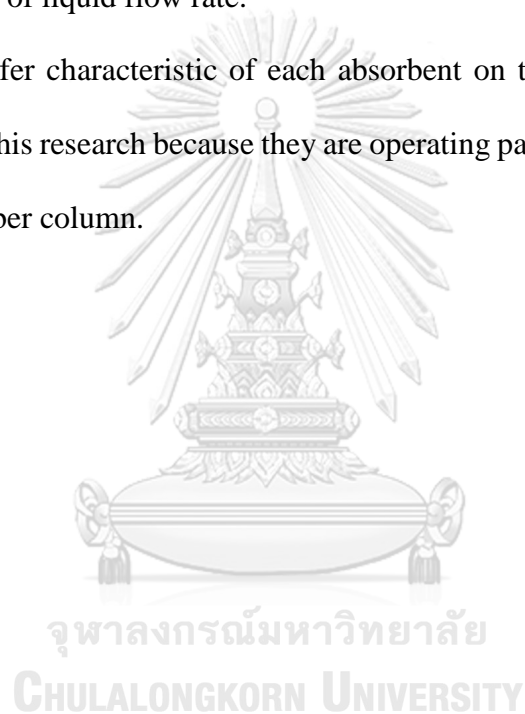
Also, effect of solution concentration, inert gas flow rate and liquid flow rate are usually examined. The study of Maneeintr et al. [17] in which volumetric mass transfer coefficient between MEA and DEAB were compared in a DX structured packed column showed that an increase in solvent concentration of both MEA and DEAB also enhanced mass transfer coefficient. Greater concentration resulted in greater free amine molecules that could capture CO₂ than lean concentration. However, higher concentration of solution would cause higher rate of corrosion and heat regeneration in heat exchanger. Liquid viscosity also increased causing pump to work harder. This also agreed with the study of Aroonwilas et al. [16] and Naami et al. [19].

Liquid flow rate also had an effect on CO₂ absorption. An increase in liquid flow rate resulted in higher free amine molecules to absorb CO₂, higher gas-liquid contact area and higher liquid side mass transfer (k_L), all of which led to higher mass transfer coefficient as described in the study of Maneeintr [17], Aroonwilas [16] and

Naami [19]. Despite of higher mass transfer, an increase in liquid flow rate affected design parameters - column diameter, absorbent circulation rate and heat regeneration cost.

From previous studies, inert gas flow rate did not have any significant effect on mass transfer characteristics because gas-side mass transfer coefficient was not a controlling-factor but a liquid-side mass transfer coefficient instead. This agreed with the study on effect of liquid flow rate.

Mass transfer characteristic of each absorbent on these described parameters will be studied in this research because they are operating parameters that are important in full-scale absorber column.



CHAPTER 3

EXPERIMENT

This chapter provides information on experimental procedure of packed absorption operation, solvent concentration and CO₂ loading calculation and scope of investigation.

3.1 Chemicals

For gas phase, 99.6% purity Nitrogen (industrial grade) was obtained from Praxair. Carbon dioxide with purity of 99.6% was also obtained from Praxair. For liquid phase, Monoethanolamine purity 99.9% was purchased from DOW chemical. 2-(Methylamino)ethanol and Dimethylaminoethanol with the same purity of 99.9% were purchased from Merck. All chemicals were used as received without purification.

3.2 Experimental method

3.2.1 Packed column operation

CO₂ and N₂ were separately fed through needle valves before passing mass flow meter (CO₂ 0-5 L/min and N₂ 0-10 L/min, Aalborg). Then, two gases were merged to form simulated gas before being supplied into the column via gas inlet line. IR analyzer with CO₂ 0-20 v/v% range (IEQ Chek, Bacharach) was equipped to measure CO₂ content in both fresh gas stream and each sampling point along the length of the column. There were eleven sampling points in total, where the first five sampling points at bottom were ten centimeters apart and other six sampling points were twenty

centimeters from one another. At each point, pressure gauge (0-2 kg/cm², Imari), temperature probe (Type K, KTT320, Kimo) and sampling outlet were embedded into the column. Inlet flow to CO₂ analyzer should be limited between 0.3-0.5 L/min in order to operate normally and cause no error. Diaphragm pump (5.5 L/min, Laboport) was applied to suck gas sample and to reduce pump duty of CO₂ analyzer. Therefore, rotameter (100-1000 CC/min, New Flow) was equipped to measure inlet gas flow rate. Three-way valve was equipped to split and ventilate excess flow to atmosphere. For liquid side, alkanolamine (MEA, 2-MAE and DMAE) was pumped through adjustable pump speed peristaltic pump (60-600 rpm, BT600-2J, Longer) and PTFE rotameter (0-200 mL, Cole-Palmer) according to 0.04-0.12 L/min of solvent flow rate. Steady state was reached when liquid flow rate outlet was constant and CO₂ content measured by CO₂ analyzer was constant. When steady state was reached, concentration of CO₂ in gas phase at each sampling point would be measured by IR analyzer. Mixed gas was drawn from inside the column and passed through narrow tube so that liquid droplet accompanying with gas would gravitationally drop by water trap, so only gas could be measured by IR analyzer. Moreover, sampling points were designed with an incline of 45° to ground level to enhance liquid trap. Liquid flow rate could be recalculated by measuring volume of liquid outlet in a cylindrical beaker for a specified time. CO₂ concentration in liquid phase could be measured by titration method as described in detail in the next section. Schematic diagram of experimental equipment is depicted in Figure 3.1.

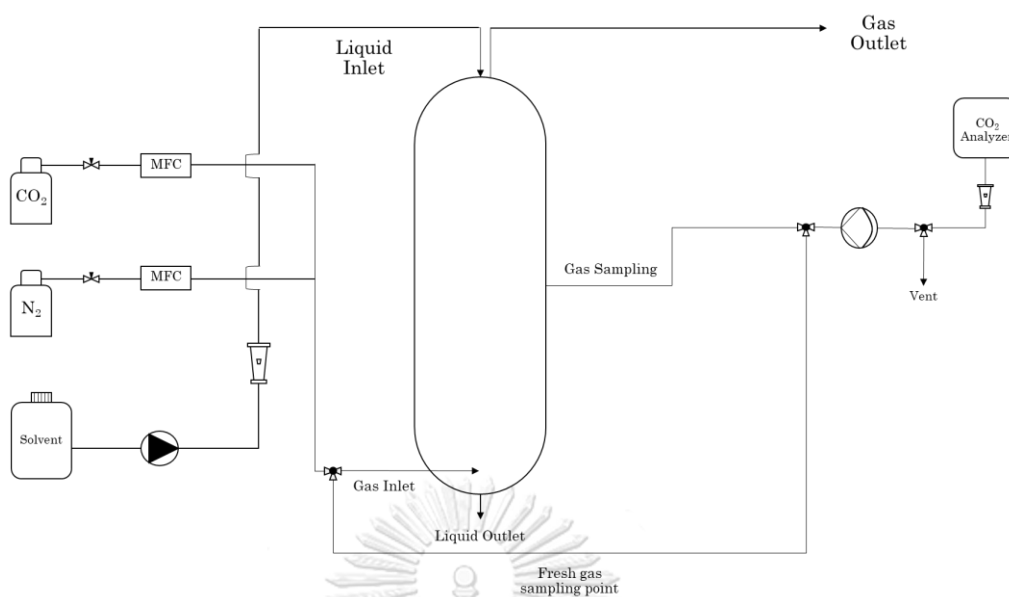


Figure 3.1 Experimental setup

3.2.2 Solvent concentration and CO₂ loading calculation

Solvent concentration and CO₂ loading could be calculated from this equipment. To calculate amine concentration, 2 mL of solvent was taken and titrated with 1 M HCl. Methyl orange was used as an indicator. Once the indicator turned from orange to red, volume of HCl in burette was recorded to calculate concentration of amine based on the principle that the end point of titration is where the equal molar of HCl reacts with OH⁻ in amine.

$$[\text{RNH}_2]V_{\text{RNH}_2} = [\text{HCl}]V_{\text{HCl}}$$

Since 2 mL of solvent and 1 molar of HCl were used in all cases, therefore concentration of RNH₂ would be expressed as Equation (3.1)

$$[\text{RNH}_2] = \frac{V_{\text{HCl}}}{2} \quad (3.1)$$

For CO₂ loading capacity, set of equipment as illustrated in Figure 3.2 was applied to determine CO₂ loading capacity. First, a sample flask was tightly placed underneath HCl burette and check for leak. Then, HCl was slowly introduced into the sample flask until reached the end point. At this point, V_{HCl} was recorded and the concentration could be calculated according to Equation 3.1. Afterward, two times of amount of V_{HCl} was supplied into the flask to ensure that all dissolved CO₂ were desorbed from the solution (V_{HCl,excess}). Amount of CO₂ releasing from the solution (V_{gas}) was recorded by amount of gas reading in the tube with non-physically or chemically CO₂ soluble substance. Therefore, volume of CO₂ dissolved in amines (V_{CO₂}) could be given by Equation (3.2)

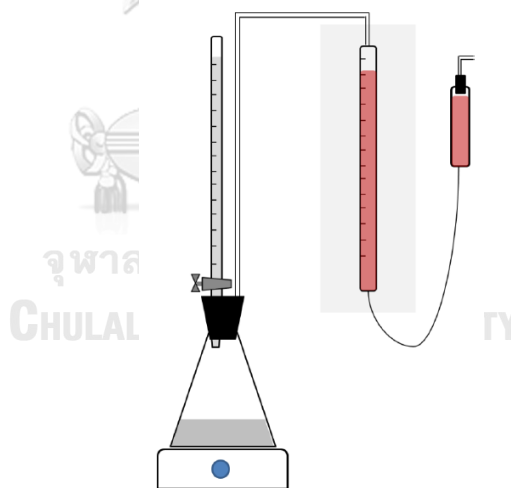


Figure 3.2 CO₂ loading analyzer

$$V_{\text{CO}_2} = V_{\text{gas}} - V_{\text{HCl,excess}} \quad (3.2)$$

To calculate mole of CO₂, ideal gas law is applied. At standard temperature and pressure (STP), mole of CO₂ could be written as below

$$\text{mole of CO}_2 (0^\circ\text{C}, 1 \text{ atm}) = \frac{V_{\text{CO}_2}}{RT} = \frac{V_{\text{CO}_2}}{0.08206 \times 273} = \frac{V_{\text{CO}_2}}{22.4}$$

Therefore, CO₂ loading at STP could be expressed by dividing mole of CO₂ by mole of amine given from titration.

$$\text{CO}_2 \text{ loading} = \alpha_{\text{STP}}(0^\circ\text{C}, 1 \text{ atm}) = \frac{V_{\text{CO}_2}}{22.4V_{\text{HCl}}}$$

At room temperature and pressure (25°C and 1 atm), CO₂ loading capacity could be calculated from Equation (3.3)

$$\alpha(25^\circ\text{C}, 1 \text{ atm}) = \frac{(V_{\text{gas}} - V_{\text{HCl,excess}})}{22.4V_{\text{HCl}}} \times \frac{273}{298} \quad (3.3)$$

3.3 Scope of experiment

As proposed in Section 1.6, scope of this study is shown in Table 3.1

Table 3.1 Scope of investigation

Variable	Range of investigation
Type of alkanolamine	MEA, 2-MAE, DMAE
CO ₂ inlet loading capacity, mol/mol	0.0, 0.1, 0.2
Concentration of solvent, kmol/m ³	3.0, 4.0, 5.0
Solvent flow rate, m ³ /(m ² ·h)	5.3, 10.6, 15.9
CO ₂ concentration in gas phase, v/v%	13, 14, 15

CHAPTER 4

RESULTS AND DISCUSSION

In this chapter, reaction regime of CO₂-amine system would be identified so that enhancement factor and its related parameter would be chosen in relation to the regime. Dependence of solvent types, CO₂ inlet loading in solvent, solvent concentration, solvent flow rate and CO₂ concentration in bulk gas on overall mass transfer coefficient based on volumetric unit of absorption ($K_G a_v$) of MEA, 2-MAE and DMAE would be discussed.

4.1 Reaction regime

With the concept of enhancement factor (I) discussed in Section 2.4, if $I > 1$ the enhancement factor would promote mass transfer in liquid film according to Equation (2.14). As a consequence, overall mass transfer coefficient would be larger.

$$\frac{1}{K_G} = \frac{1}{k_G} + \frac{H}{Ik_L^0} \quad (2.14)$$

O. Levenspiel [28] introduced the concept of Hatta Number (Ha) which is a dimensionless number invented by Shiroji Hatta and enhancement factor to define which reaction regime of the interested system would fall in. Ha is the comparison between conversion of reactant in liquid film and molecular diffusion through the film. Ha Number for CO₂-MEA system is represented below by Equation (4.1)

$$Ha^2 = \frac{k_{CO_2,i} c_{MEA} x}{D_{CO_2,MEA} c_{CO_2,i}} = \frac{k_{MEA} D_{CO_2,MEA}}{(k_L^0)^2} \quad (4.1)$$

where k is rate of reaction constant, $D_{CO_2,MEA}$ is diffusivity of CO_2 in MEA, c_{MEA} is concentration of MEA in bulk liquid and x is distance that CO_2 molecules travel into liquid film. According to penetration theory [25], k_L^0 is proportional to square root of diffusivity where t_c is a contact time between gas and liquid.

$$k_L^0 = 2 \sqrt{\frac{D_{CO_2,MEA}}{\pi t_c}} \quad (4.2)$$

Substitute k_L^0 from Equation (4.2) in Equation (4.1) yields

$$Ha = \sqrt{\frac{\pi}{4} k_{MEA} t_c} \quad (4.3)$$

For our study, $k=2,187.3 \text{ m}^3/(\text{kmol}\cdot\text{s})$ at MEA concentration $3\text{-}9 \text{ kmol/m}^3$ 298 K [15], $c_{MEA}=3 \text{ kmol/m}^3$ and $t_c=73.08 \text{ s}$. According to the Equation (4.3), $Ha=613.7$. For enhancement factor, the comparison between rate of CO_2 loss by reaction and rate of CO_2 loss by molecular diffusion could be shown in Equation (4.4) [28].

$$I_i = 1 + \frac{D_{MEA} c_{MEA} H_{CO_2-MEA}}{D_{CO_2} p_{CO_2,i}} \quad (4.4)$$

where $D_{MEA}/D_{CO_2}=0.389$ [25, 29], $H_{CO_2-MEA} = 4,325.48 \text{ (kPa}\cdot\text{m}^3)/\text{kmol}$ (see Section 4.6) $c_{MEA}=3 \text{ kmol/m}^3$ and $p_{CO_2,i}=0.15 \times 10^5 \text{ kPa}$ (CO_2 content 15 v/v%)

where partial pressure of CO₂ was assumed to be equal in the bulk gas. Therefore, $I_1=334.19$.

If $5I_1 > Ha > \frac{I_1}{5}$ this reaction would occur in liquid film and all CO₂ would be consumed before leaving liquid film [28] leading to $y_{CO_2}^*=0$. Also, this reaction falls in fast reaction regime which states in Astarita et al. [22] that enhancement factor would be an inverse function of reaction time (t_r) which is reaction time for CO₂ to be absorbed in liquid film as in Equation (4.5).

$$I \propto t_r^{-0.5} \quad (4.5)$$

Reaction between CO₂ and amines in liquid film taking place at the wetted surface of packing should be similar to Figure 4.1. At gas-liquid interface, dissolved CO₂ reacted with diffusing amines and depleted within liquid film before transferring into bulk liquid. Therefore, no reaction occurred in bulk liquid. With this concept, overall mass transfer coefficient based on gas phase would be a promising representative of overall mass transfer coefficient for absorber column since liquid film resistance was a dominant one and gas film resistance was negligible. Moreover, in general gas treating process, gas phase composition along the height of column is an interested parameter rather than liquid phase composition.

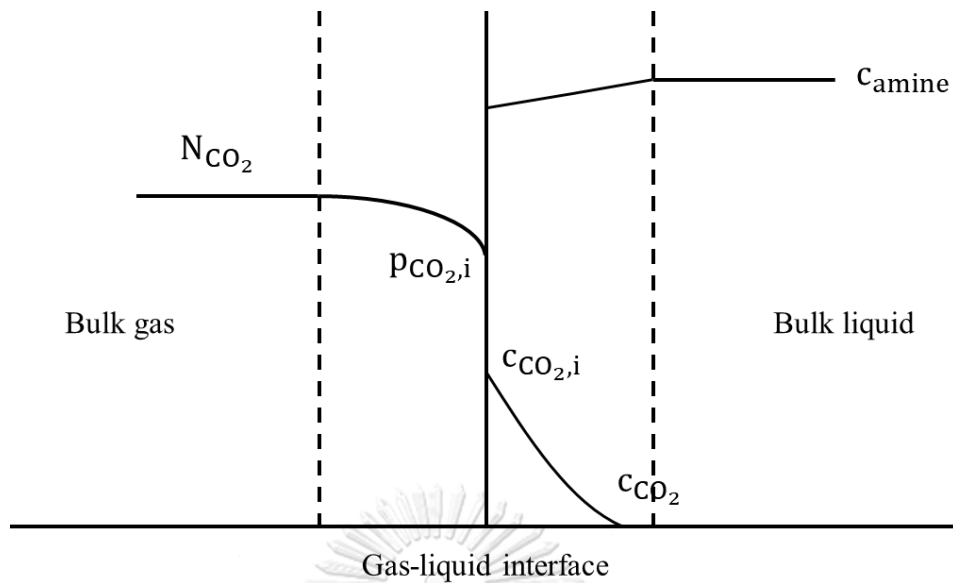


Figure 4.1 CO₂ reaction in liquid film for fast reaction regime

4.2 Effect of solvent types

Mass transfer coefficient of MEA, 2-MAE and DMAE were investigated in order to compare dependence of alkanolamine types which are primary, secondary and tertiary on mass transfer coefficient. Experimental was conducted at solvent concentration of 3 kmol/m³, CO₂ concentration in bulk gas 15 v/v%, CO₂ inlet loading in solvent 0.200 mol/mol, solvent flow rate 10.6 m³/(m²·h) and total gas flow rate of 4 L/min. Comparison of $K_G a_v$ for each solvent is shown in Figure 4.2.

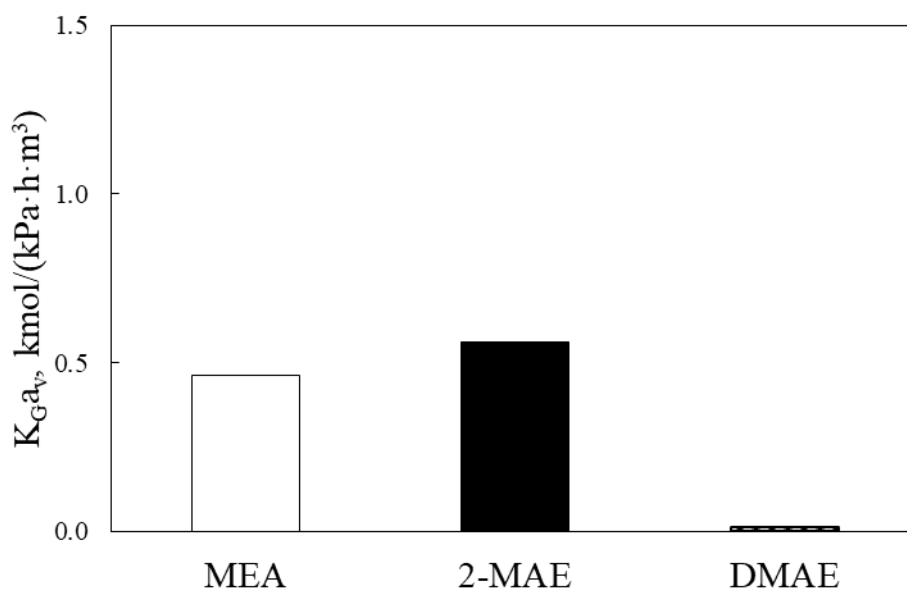


Figure 4.2 Overall mass transfer coefficient of MEA, 2-MAE and DMAE

As shown from Figure 4.2, 2-MAE performs the highest $K_G a_v$ of 0.5622, while MEA and DMAE show lower $K_G a_v$ of 0.4638 and 0.0137, respectively. $K_G a_v$ value of 2-MAE is 121% higher than that of MEA and upto 4104% than DMAE. The major difference among three solvents is their chemical structure. 2-MAE and DMAE exhibit a methyl group and two methyl group, respectively, as suggested in Table 2.2. Alkanolamine possess both hydroxyl and amine group in which hydroxyl group played a role to enhance solubility of amine into water and reduce vapor pressure to increase the boiling point for regeneration purpose. On the other hand, amine group enhanced basicity of solvent in order to react with dissolved CO_2 [14].

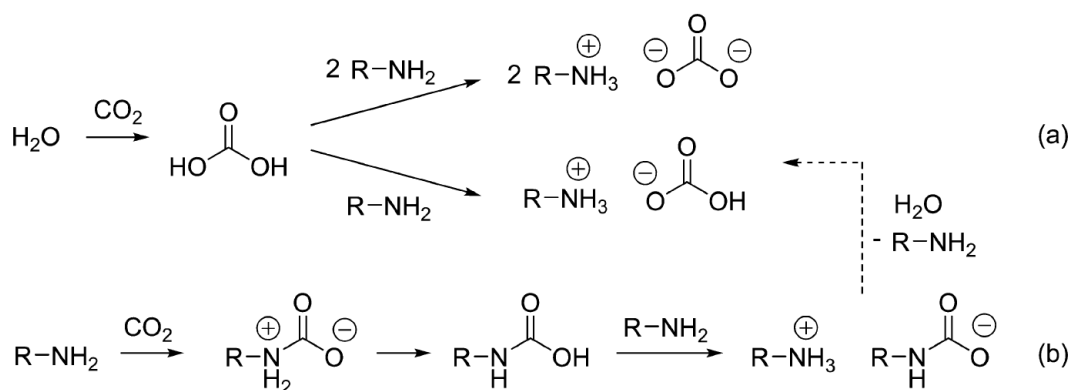


Figure 4.3 Reaction pathway of primary, secondary and tertiary amines [30]

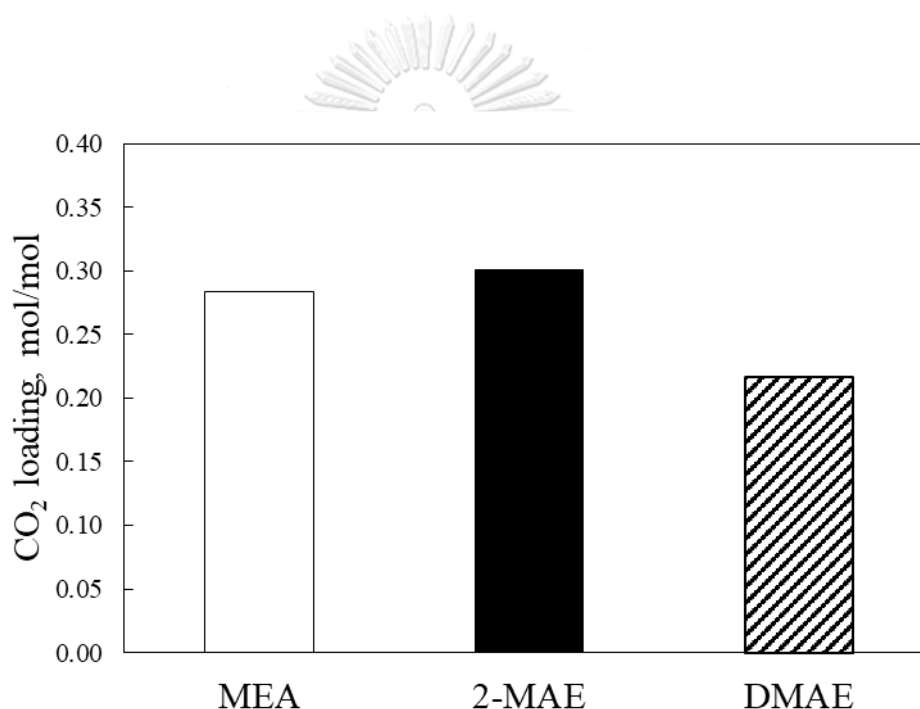


Figure 4.4 CO_2 outlet loading of MEA, 2-MAE and DMAE

Reaction pathway of primary, secondary and tertiary amines is shown in Figure 4.3 for more detail. Reaction pathway (a) belonged to all three types of amines. Since there was no proton in their molecules, tertiary amines work only as a proton acceptor and cannot directly react with CO_2 [30]. For pathway (a), CO_2 dissolved in water forming carbonic acid, then amine would perform as a Bronsted base (electron donor

or in other word proton acceptor) to lessen acidity of carbonic acid [30]. This path could proceed in two ways in which ammonium carbonate or ammonium bicarbonate were formed. Reaction path (b) is for primary and secondary amines forming zwitterion before deprotonated and yielded carbamic acid. Then, another free amine molecule collided with carbamic acid leading to ammonium and carbamate formation. With hydrolysis of water, bicarbonate was created [30].

In our case, DMAE which is a tertiary amine followed path (a) and proceeded toward carbonate/bicarbonate formation. Kortunov et al. suggested that carbonic formation was a rate limiting step for carbonate/bicarbonate formation at room temperature and pressure [30]. From Figure 4.3, it could be seen that hypothetically ratio of CO₂: amine was 1:1 in case of bicarbonate, but could be 2:1 in case of carbonate formation. Though, theoretically, equilibrium solubility of DMAE could be as high as 1:1 which is the highest among three amines. Figure 4.4 shows that CO₂ loading outlet of DMAE is 0.217, relatively small compared to MEA and 2-MAE which are 0.284 and 0.301, respectively. This would be a result of too short contact time in the column to reach equilibrium condition together with slow rate of reaction of tertiary amine. Also, at early stage of absorption, carbonate was equivalently produced as bicarbonate. Thus, only 0.017 mole of CO₂ per mole of amine was absorbed into DMAE which was rather low, regarding its full capacity of CO₂ solubility [30].

On the contrary, MEA and 2-MAE followed reaction path (b) and formed carbamate and ammonium ion. By following this path, ratio of CO₂: amine at equilibrium was literally 1:2 despite solubility of 2-MAE and MEA stated otherwise [24], [23] because hydrolysis reaction between water and carbamate occurred leading to bicarbonate formation and left a free amine molecule from the reaction. Bicarbonate

could be produced as in path (a) as well even if reaction rate via carbonic acid formation was relatively slow compared to zwitterion [15] so, for MEA and 2-MAE, bicarbonate was mostly produced via zwitterion and hydrolysis. Reaction rate between primary and secondary amines are competitive [30] but 2-MAE exhibited lower carbamate stability than MEA as a result of its methyl group causing inferior electrophilicity over MEA [30]. Moreover, Gangarapu et al. reported that 2-MAE exhibited lower carbamate stability than MEA due to lower Gibbs energy for the carbamate hydrolysis reaction of 4.80 and 5.83 kcal/mol, respectively [31]. Therefore, carbamate formed in 2-MAE-CO₂ system was hydrolyzed and formed bicarbonate resulting in higher CO₂ absorption per mole of amine and reaction moved toward product (carbamate formation) according to Equation (2.5). These led to higher rate of mass transfer in 2-MAE over MEA. Moreover, carbamate hydrolysis released a free amine molecule to capture CO₂ once again.

Table 4.1 pK_a value of solvents

Alkanolamine	pK _a	Reference
Monoethanolamine	9.16	[30]
2-(Methylamino)ethanol	9.40	[30]
Dimethylaminoethanol	8.88	[30]

Table 4.1 represents each solvent's pK_a value. pK_a is an acid dissociation constant. If pK_a is small, solution exhibits high acidity. With this knowledge, one could roughly predict basicity of amines. In contrast, Li et al. reported that solvents with low pK_a tended to show larger K_Ga_v due to reaction toward product side [13]. However, results from this study showed that, even though pK_a was high causing forward rate to

product to be higher, it was still competitive in case of MEA and 2-MAE. Carbamate stability played an important role in CO₂ capture efficiency.

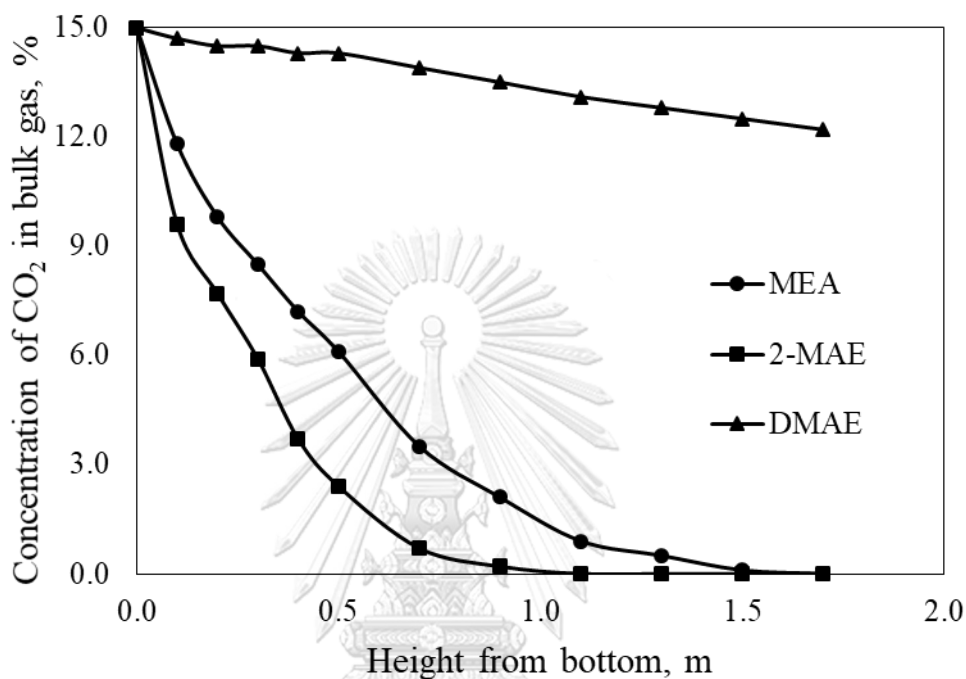


Figure 4.5 CO₂ concentration in bulk gas of MEA, 2-MAE and DMAE against height

Figure 4.5 reveals that at the same height of the column, 2-MAE absorbs largest amount of CO₂ representing lowest amount of remaining CO₂ in bulk gas phase. On the other hand, MEA and DMAE show higher remaining CO₂ molecules compared at the same level. According to the figure, 2-MAE captures all CO₂ since 0.90 m from bottom of the column while, in case of MEA, CO₂ is depleted at 1.5 m and consequently needed 66.7% of height to achieve 100% CO₂ removal efficiency as 2-MAE did. However, in case of DMAE, overall CO₂ efficiency was just 18.7%.

In addition, regeneration of amines required input energy to break N-C bond in order to desorb CO₂ from carbamate, bicarbonate and carbonate [30]. As mentioned

earlier, MEA exhibits disadvantage on high energy consumption which was a result of carbamate stability in primary amines. Regarding to this matter, 2-MAE was a good candidate with higher mass transfer coefficient, CO₂ capture capacity and requiring lower heat of regeneration due to reduced carbamate stability. DMAE performed the lowest energy consumption among three amines, and exhibited least CO₂ removal efficiency since its slow rate of reaction in carbonic formation step.

4.3 Effect of CO₂ inlet loading

MEA, 2-MAE and DMAE were examined at the same condition which included solvent concentration at 3 kmol/m³, solvent flow rate at 10.6 m³/(m²·h), CO₂ content at 15 v/v% and total gas flow rate fixed at 4 L/min in order to compare effect of CO₂ inlet loading in absorbent at 0.0, 0.1 and 0.2 mol/mol for each solvent type.

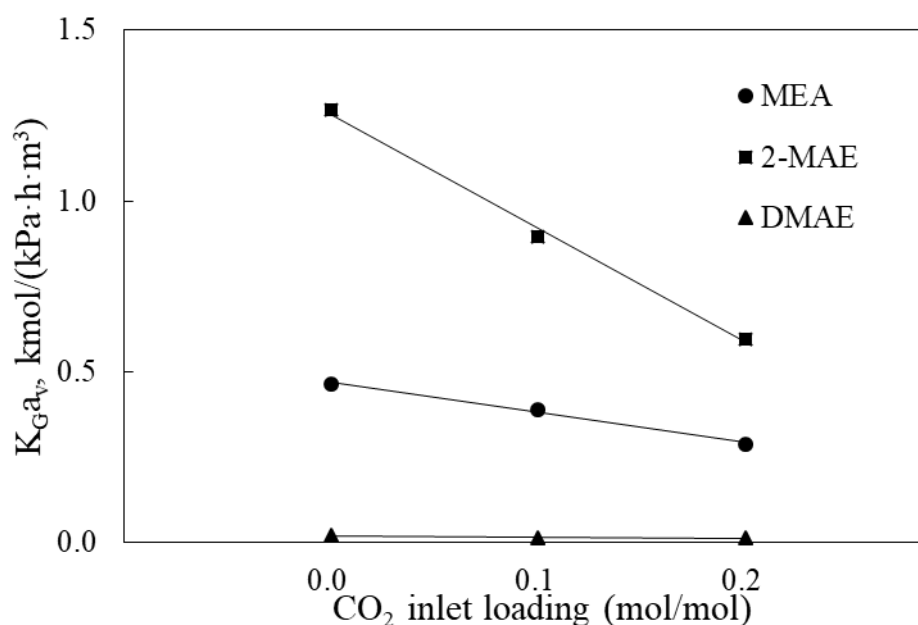


Figure 4.6 Overall mass transfer coefficient of MEA, 2-MAE and DMAE at CO₂ inlet loading of 0.0, 0.1 and 0.2 mol/mol

Figure 4.6 shows that, at CO₂ inlet loading range from 0.0 to 0.2 mol/mol, 2-MAE performs the highest K_Ga_v among three amines followed by MEA and DMAE, respectively. Regarding to the slope of each trend line, an increase in CO₂ inlet loading from 0.0 to 0.2 mol/mol causes a significant drop in K_Ga_v in case of 2-MAE while MEA and DMAE exhibit less decline as shown in Table 4.2.

Table 4.2 K_Ga_v of solvents at each CO₂ inlet loading capacity

mol/mol	K _G a _v , kmol/(kPa·h·m ³)		
	MEA	2-MAE	DMAE
α=0.0	0.4638	1.2656	0.0215
α=0.1	0.3908	0.9698	0.0139
α=0.2	0.2880	0.5654	0.0137
Slope	0.879	3.501	0.039

Dependence on CO₂ inlet loading could be explained by kinetic mechanism, as earlier reported in Section 4.1. CO₂ absorption mechanism could be written as in Equation (2.1) and (2.2) for primary and secondary amines (MEA and 2-MAE) and Equation (2.3) for tertiary amines (DMAE). As described in Section 4.2, though Equation (2.3) occurred in case of MEA and 2-MAE, rate constant was comparatively sluggish compared with Equation (2.1) and (2.2).



From basic knowledge, rate of reaction depends on reactant concentration. Also, Arrhenius's Law points that reaction constant (k) depends on reactant nature and system

temperature as shown in Equation (4.6). In this study, system temperature was assumed to be constant in all cases.

$$k = k_0 e^{\frac{-E_a}{RT}} \quad (4.6)$$

Therefore, in Equation (2.1) and (2.2), if the concentration of RNH_2 was high, forward rate of reaction would also be rapid leading to more absorption of molecules of CO_2 into amines. Comparison between unloaded ($\alpha=0.0$), or fresh, and preloaded amines ($\alpha=0.1$ and 0.2), preloaded amines clearly exhibited molecules on the product side (RNHCOO^- , RNH_3^+ , H^+ , HCO_3^-) before reaction would take place while the unloaded solvent did not due to no available CO_2 molecules in the solvent. Thus, unloaded amine would produce higher rate of reaction due to higher concentration of RNH_2 and consequently absorbed more molecules of CO_2 at the same level. Therefore, 2-MAE at $\alpha=0.0$ would give higher value of $K_G a_v$ than those of $\alpha=0.1$ and 0.2 (This also applied when compare $\alpha=0.1$ with 0.2).

Evidence gaining from titration (see Table 4.3) before and after experiment showed that all three solvents consumed 6 mL of HCl to reach the end point which indicated that they still contained the equivalent concentration of amine to react with HCl. Total concentration of $-\text{NH}_2$ and $-\text{NH}$ groups in MEA and 2-MAE, respectively, are comprised of three parts (I) RNH_2 , (II) RNHCOO^- and (III) RNH_3^+ . Therefore, a decrease in reactant RNH_2 would lead to an increase in RNHCOO^- and RNH_3^+ . At $\alpha=0.0$, there was only RNH_2 in the solution whereas at $\alpha=0.1$ some amines containing molecules were contributed to RNHCOO^- and RNH_3^+ , causing a lower amount of RNH_2

molecules. Consequently, rate of reaction which is directly influenced by reactant concentration would be slower than that of unloaded solvents.

For DMAE, similar case also applied, concentration of $-NR_2$ group contributed to R_3N and ammonium ion R_3NH^+ as described in Figure 4.3 reaction pathway (a) and also in Equation (2.3). As seen in Table 4.3, amine concentration of DMAE before and after the experiment is equal. Once DMAE absorbed CO_2 , reactant R_3N was converted into R_3NH^+ and carbonate/bicarbonate molecules, resulting in a reduction of R_3N concentration. Thus, rate of reaction of unloaded solvent was higher than that of preloaded solvent.

As stated in Section 4.1, all dissolved CO_2 molecules reacted with amine molecules and depleted in liquid film before entering bulk liquid region. Therefore, starting with the equivalent amount of dissolved CO_2 at the interface (compared with the same CO_2 -amine system at constant temperature and CO_2 partial pressure, solubility of CO_2 , according to Henry's law, should be equal), reaction time of systems with $\alpha=0.0$ would be shorter than the systems with $\alpha=0.1$ and 0.2 . This explanation also applied when $\alpha=0.1$ and 0.2 were compared. A decrease in reaction time would lead to an increase in enhancement factor and consequently resulted in larger $K_G a_v$ as stated in Equation (4.5) and (2.14), respectively.

Table 4.3 Titration of MEA, 2-MAE and DMAE before and after the experiment

	Before			After		
	MEA	2-MAE	DMAE	MEA	2-MAE	DMAE
V_{HCl} , cm^3	6.0	6.0	6.0	6.0	6.0	6.0
$V_{HCl,excess}$, cm^3	12.0	12.0	12.0	12.0	12.0	12.0
Concentration, $kmol/m^3$	3.0	3.0	3.0	3.0	3.0	3.0

In view of reaction mechanism, a significant drop of $K_G a_v$ in 2-MAE led to the fact that too high bicarbonate formation via zwitterion pathway, though enhanced CO_2 absorption efficiency, might diminish carbamate formation than the presence of carbamate itself (compared to MEA which presented more carbamate formation). Moreover, DMAE, which bicarbonate were formed via carbonic acid formation, did not give the same effect as 2-MAE. Figure 4.7 reveals that for all conditions of CO_2 inlet loading, 2-MAE still absorbs the highest amount of CO_2 from bulk gas among the studied amines. Again, the reason for this was from bicarbonate formation as suggested in Section 4.1. DMAE absorbs the lowest amount of CO_2 since its slow rate of reaction compared to others, even though performed the highest CO_2 solubility at equilibrium state [30].

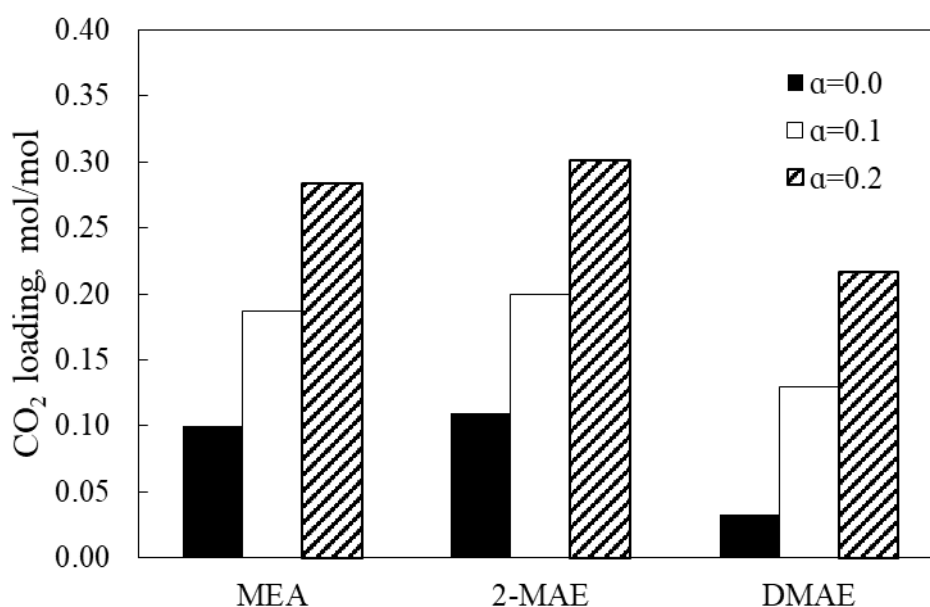


Figure 4.7 CO_2 outlet loading of MEA, 2-MAE and DMAE at CO_2 inlet loading of 0.0, 0.1 and 0.2 mol/mol

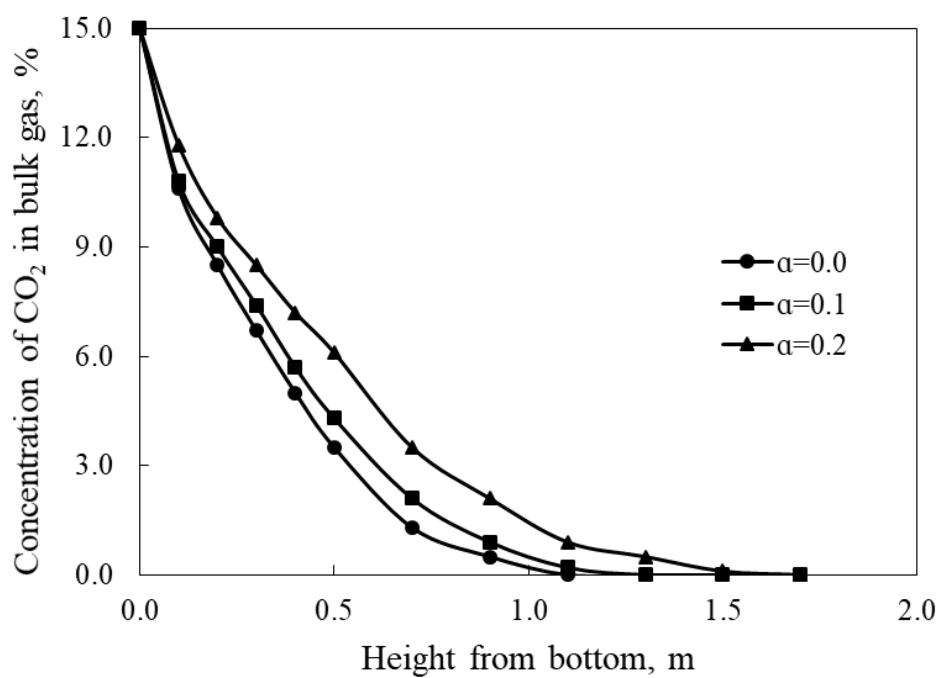


Figure 4.8 CO₂ concentration in bulk gas of MEA against height at CO₂ inlet loading of 0.0, 0.1 and 0.2 mol/mol

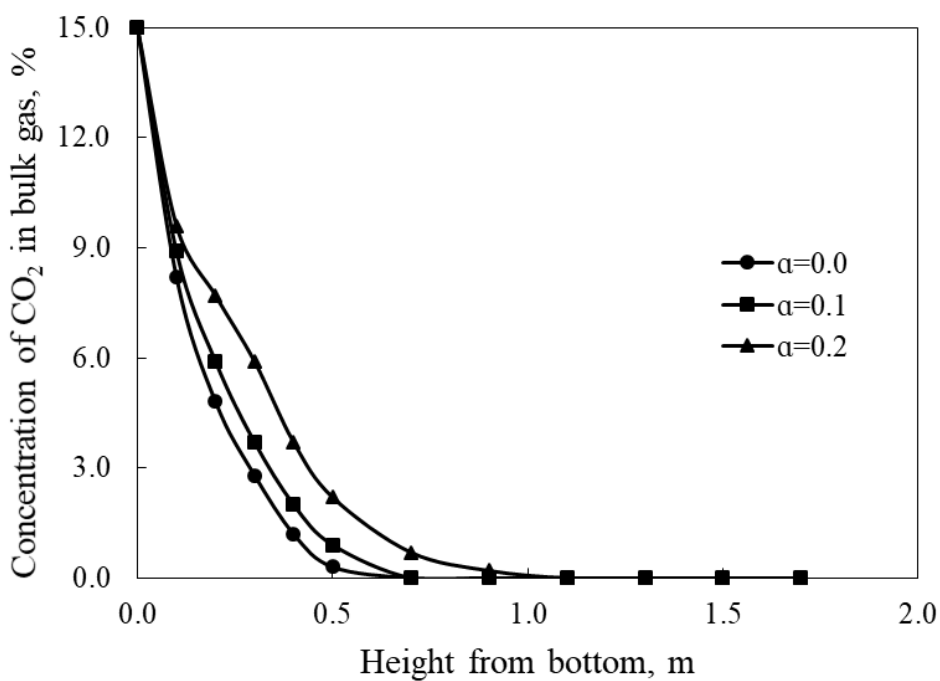


Figure 4.9 CO₂ concentration in bulk gas of 2-MAE against height at CO₂ inlet loading of 0.0, 0.1 and 0.2 mol/mol

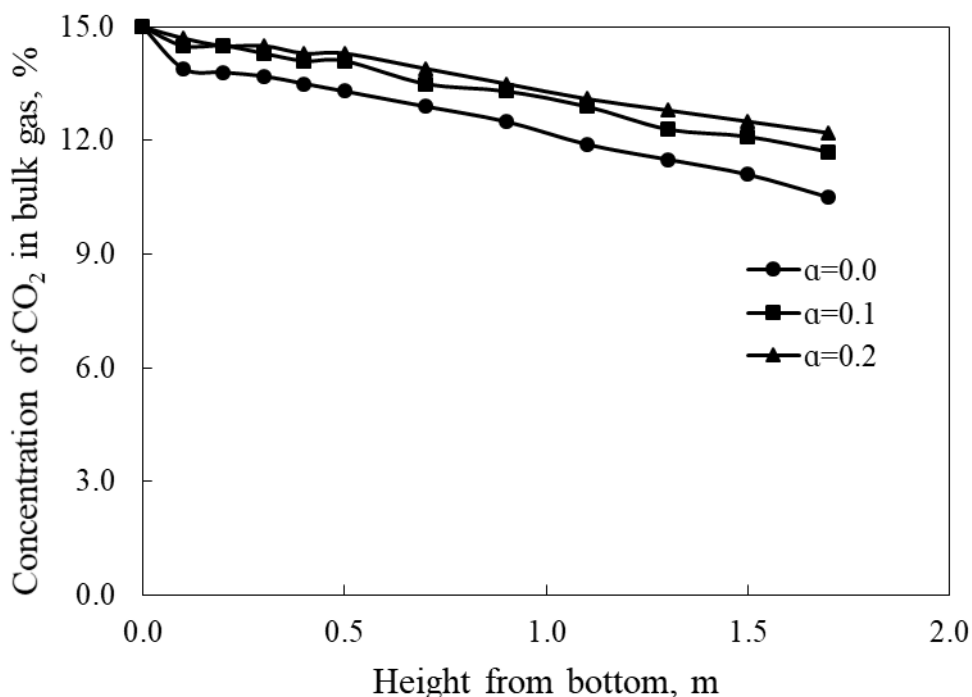


Figure 4.10 CO₂ concentration in bulk gas of DMAE against height at CO₂ inlet loading of 0.0, 0.1 and 0.2 mol/mol

Figure 4.8, 4.9 and 4.10 display CO₂ concentration in bulk gas of MEA, 2-MAE and DMAE analyzed by IR analyzer along the length of the column at CO₂ inlet loading of 0.0, 0.1 and 0.2 mol/mol. As shown in Figure 4.7 and Figure 4.9, as CO₂ inlet loading increases, MEA and DMAE absorb less CO₂ because preloaded solvents exhibited lower RNH₂ and R₃N. 2-MAE also follows the same trend as MEA and DMAE. CO₂ concentration in bulk gas of 2-MAE at α=0.2 obviously shows higher value than at α=0.0 and 0.1 which conforms to the significant drop in K_Ga_v due to bicarbonate formation. Comparison of CO₂ removal efficiency suggested that 2-MAE at α=0.0 could absorb all CO₂ since 0.7 m. Also, at α=0.1, 2-MAE absorbs all CO₂ at the same level of 0.7 m because the remaining reactant concentration could capture CO₂ in gas phase within 0.2 m distance of sampling point. At α=0.2, CO₂ removal efficiency

reaches 100% at 1.1 m, which was 57% of height more than at $\alpha=0.1$. In case of MEA, at $\alpha=0.0$, CO₂ becomes exhausted at 1.1 m while, at $\alpha=0.2$, CO₂ is depleted at the top of the column (1.7 m) requiring 55% more height to achieve the same level of efficiency. With slow rate of reaction, despite the highest $K_G a_v$ of 0.0215 kmol/(kPa·h·m³) that DMAE could achieve at $\alpha=0.0$, CO₂ removal efficiency at the exit is only 30%. Obviously, unloaded solvent performed higher mass transfer rate than preloaded one. Though 2-MAE performed the highest $K_G a_v$ in all conditions, the considerable drop when CO₂ inlet loading increased should be noted. Nevertheless, in regeneration unit, it is impossible to desorb all CO₂ from the solvent, of which inlet feed contained CO₂ loading of approximately 0.1-0.3 mol/mol [32].

To achieve high mass transfer rate, lower inlet CO₂ loading is preferred. However, to gain low CO₂ loading capacity, large energy would be consumed in order to desorb more CO₂ molecules from absorbent. The higher the regeneration temperature is the more CO₂ desorption the regeneration process achieves. CO₂ desorption temperature is usually in the range of 80-150°C (8 bar) [20] so that balance between process efficiency and economic feasibility becomes optimized.

According to Artanto et al. [33], energy balance equation on reboiler heat duty could be simplified into Equation (4.7). The equation contained three major terms controlling reboiler heat duty (kJ/kg) which were heat required to evaporate water ($Q_{\text{condensor}}$), heat required to heat absorbent to regenerated temperature ($Q_{\text{absorbent}}$) and heat required to desorb CO₂ molecules from absorbent ($Q_{\text{desorption}}$).

$$Q_{\text{reboiler}} = Q_{\text{condensor}} + Q_{\text{absorbent}} + Q_{\text{desorption}}$$

$$Q_{\text{reboiler}} = m_w \Delta H_w + m_a c_{p,a} (T_{\text{bottom}} - T_{\text{top}}) + m_{\text{CO}_2} \Delta H_{\text{CO}_2} \quad (4.7)$$

where m_w was amount of water (kg), ΔH_w was latent heat of water condensation (kJ/kg), m_a was amount of solvent (kg), $c_{p,a}$ was specific heat capacity of solvent which, for simplicity, assumed constant (kJ/kg·K), T_{top} was inlet solvent temperature from the top of regeneration tower (K), T_{out} was outlet solvent temperature from bottom of regeneration tower or regeneration temperature (K), m_{CO_2} was amount of CO_2 leaving regeneration tower at the top (kg) and ΔH_{CO_2} was enthalpy of CO_2 desorption.

As stated in Equation (4.7), it could be seen that if regeneration temperature was increased, $Q_{absorbent}$ would significantly increase. For example, if regeneration temperature was changed from 80°C to 100°C, approximately 20 times of heat consumption in term of $Q_{absorbent}$ would be required. McCann et al. reported that enthalpies of CO_2 absorption and desorption strongly relied on each absorbent molar ratio of CO_2 to amine [34]. All absorbents in the study exhibited the same trend that low molar ratio (1 mol of amine captures less than 1 mol of CO_2) demanded higher heat than high molar ratio. Accordingly, to attain small value of α , one needed to consider heat consumption in term of $Q_{absorbent}$ and $Q_{desorption}$. Economically, balancing between fixed costs (tower sizing, pump, reboiler, etc.) and operating costs (solvent circulation rate, regeneration temperature, etc.) should be carefully considered in order to optimize cost and process efficiency.

4.4 Effect of solvent concentration

MEA, 2-MAE and DMAE were examined at the same condition with CO₂ inlet loading at 0.2 mol/mol, solvent flow rate at 10.6 m³/(m²·h), CO₂ content at 15 v/v% and total gas flow rate fixed at 4 L/min in order to compare effect of solvent concentration at 3, 4 and 5 kmol/m³ for each solvent type.

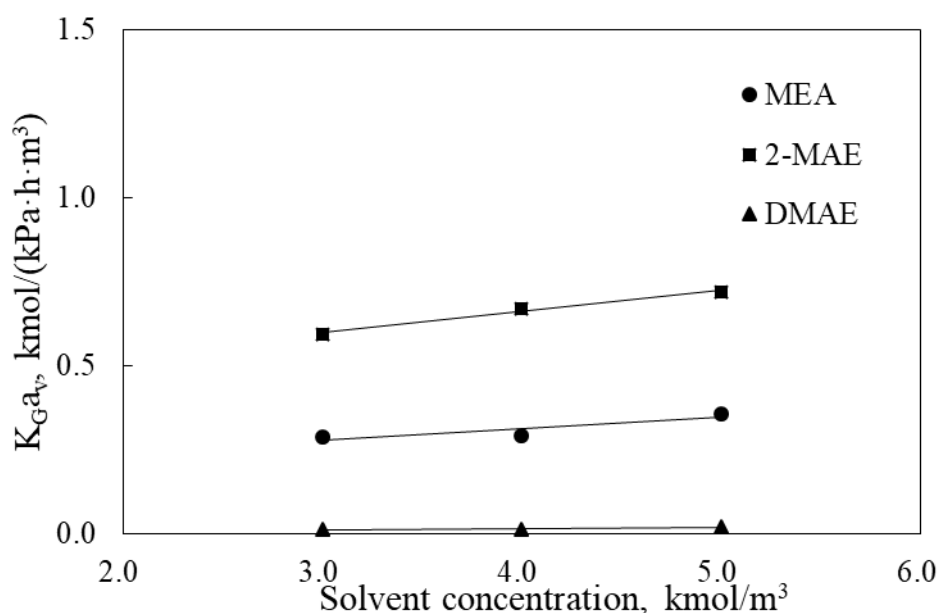


Figure 4.11 Overall mass transfer coefficient of MEA, 2-MAE and DMAE at solvent concentration of 3, 4 and 5 kmol/m³

Figure 4.11 reveals that, as solvent concentration increases, $K_G a_v$ increases and 2-MAE exhibits higher mass transfer rate than the other two for all cases. Three amines gives the fastest rate of mass transfer at 5 kmol/m³. 2-MAE performs highest mass transfer coefficient at 5 kmol/m³ of 0.7211 followed by MEA at 0.3574 and DMAE at 0.0209 kmol/(kPa·h·m³).

Table 4.4 K_{Ga_v} of solvents at each solvent at 3, 4 and 5 kmol/m³

kmol/m ³	K_{Ga_v} , kmol/(kPa·h·m ³)		
	MEA	2-MAE	DMAE
3	0.2880	0.5954	0.0137
4	0.2916	0.6714	0.0137
5	0.3574	0.7211	0.0209
Slope	0.0347	0.0629	0.0036

From Table 4.4, 2-MAE exhibited the highest slope when solvent concentration was raised from 3 to 5 kmol/m³. According to Section 4.2, bicarbonate formation enhanced CO₂ absorption rate of 2-MAE over MEA and DMAE.

An increase in solvent concentration led to an increase in number of fresh amine molecules per unit volume of solvent and apparently caused higher rate of reaction. Enhancement factor and K_{Ga_v} would become larger as a consequence. In this case, all solvents were preloaded with 0.2 mol of CO₂ per mole of amine and did not exhibit mass transfer coefficient as high as 1.2656 kmol/(kPa·h·m³) of 2-MAE at 0.0 mol/mol. Each mole of preloaded amine occupied with 0.2 mole of CO₂ meaning less free amine molecules remaining in the solvent, leading to lower mass transfer rate compared to fresh solvent. According to this effect, an increase in number of free amine molecules per unit volume increased rate of mass transfer, however, CO₂ capture efficiency per mole of amine did not increase. Figure 4.12 reveals that CO₂ outlet loading of each solvent at 5 kmol/m³ was lower than at 3 kmol/m³ because though number of free amine molecules increased, forward rate of CO₂ capture did not increase linearly. Preloaded solvent consisting of product molecules yielded lower rate of reaction than unloaded one. Again, enhancement factor depended on reaction time used to consume CO₂ in liquid film as in Equation (4.6). Reasonably, more free amine molecules in case of 5 kmol/m³ would give higher rate of mass transfer.

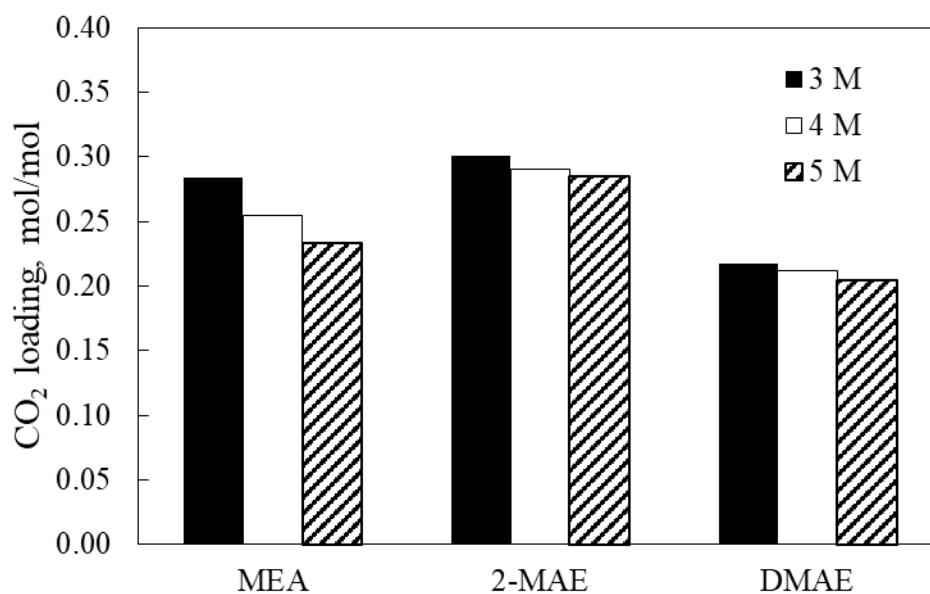


Figure 4.12 CO₂ outlet loading of MEA, 2-MAE and DMAE at solvent concentration 3, 4 and 5 kmol/m³

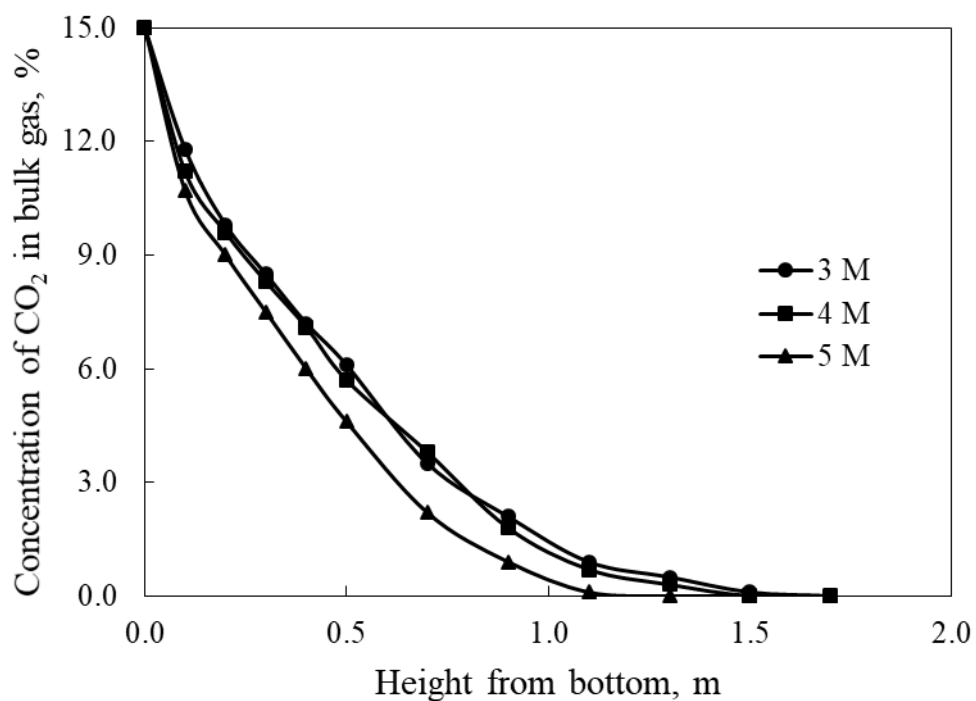


Figure 4.13 CO₂ concentration in bulk gas of MEA against height at MEA concentration of 3, 4 and 5 kmol/m³

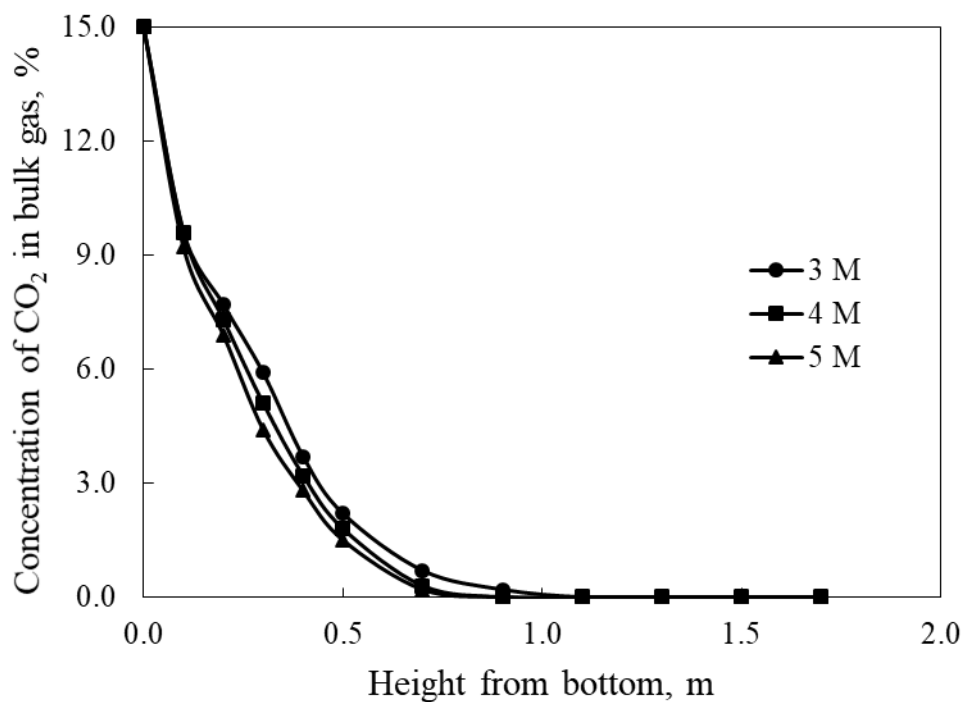


Figure 4.14 CO₂ concentration in bulk gas of 2-MAE against height at 2-MAE concentration of 3, 4 and 5 kmol/m³

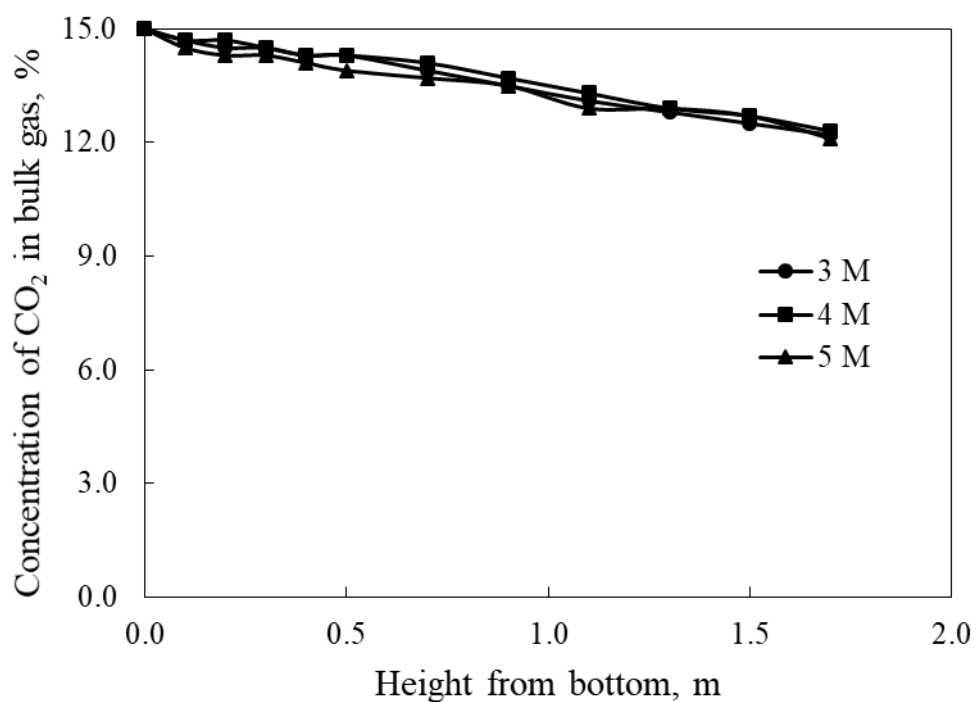


Figure 4.15 CO₂ concentration in bulk gas of DMAE against height at DMAE concentration of 3, 4 and 5 kmol/m³

Figure 4.13, 4.14 and 4.15 show that, as solvent concentration increases from 3 to 5 kmol/m³, CO₂ content in bulk gas decreases due to more free amine molecules available in the solvent to capture CO₂ from gas phase. 2-MAE absorbed all CO₂ at 0.9 m in case of 4 and 5 kmol/m³ while achieved the same efficiency at 1.1 m in case of 3 kmol/m³. On the other hand, MEA needed higher column tower to reach 100% CO₂ capture efficiency. For MEA concentration at 3, 4 and 5 kmol/m³, all CO₂ were absorbed at 1.7, 1.5 and 1.3 m, respectively. MEA exhibited lower mass transfer coefficient and consequently required higher tower to reach the same efficiency as 2-MAE. For DMAE, some of CO₂ was absorbed and the rest left the column unabsorbed. At 3, 4 and 5 kmol/m³ CO₂ capture efficiency was 18.67, 18.67 and 19.33% at the exit. Despite more free amine molecules in liquid phase, sluggish rate of DMAE still exhibited both in the case of both CO₂ inlet loading and solvent concentration.

For regeneration purpose, higher CO₂ loading capacity would lead to more energy required to desorb CO₂ from aqueous phase [34]. Therefore, solvent concentration of 5 mol/dm³ was preferred to 3 and 4 mol/dm³ because of less CO₂ loading at the outlet. In addition, Astarita et al. reported that gas treating unit using higher concentration resulted in lower overall relative cost compared to that using lower solvent concentration one [22]. However, too high solvent concentration might lead to equipment corrosion.

4.5 Effect of solvent flow rate

MEA, 2-MAE and DMAE were examined at the same condition with solvent concentration at 3 kmol/m³, CO₂ inlet loading at 0.2 mol/mol, CO₂ content at

15 v/v% and total gas flow rate fixed at 4 L/min in order to compare effect of solvent flow rate at 5.3, 10.6 and 15.9 $\text{m}^3/(\text{m}^2\cdot\text{h})$ for each solvent type.

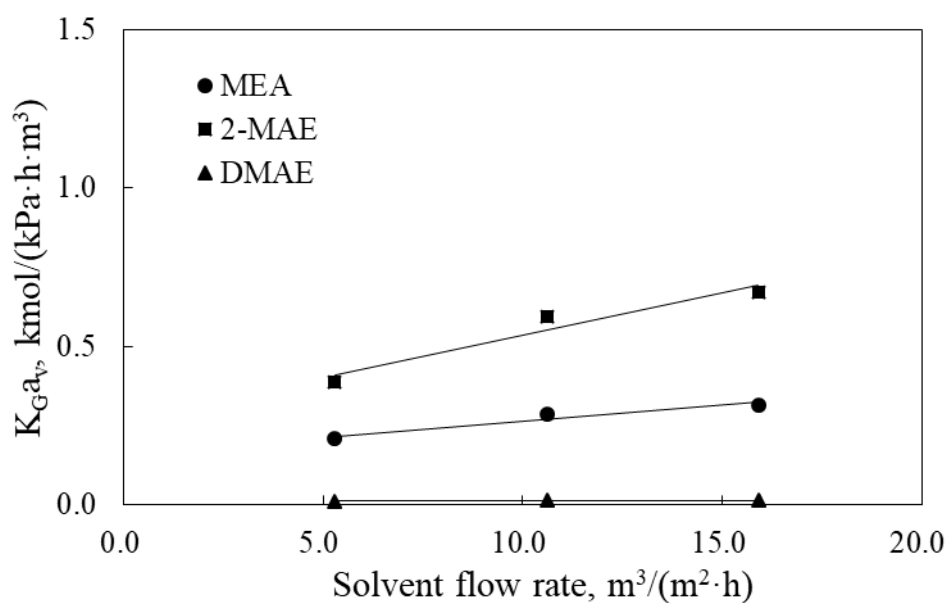


Figure 4.16 Overall mass transfer coefficient of MEA, 2-MAE and DMAE at solvent flow rate of 5.3, 10.6 and 15.9 $\text{m}^3/(\text{m}^2\cdot\text{h})$

Figure 4.16 shows that, for all three amines, $K_G a_v$ increases as flow rate increases. 2-MAE performs the highest mass transfer rate among others in the range of studied solvent flow rate followed by MEA and DMAE. Regarding to the slope of each trend line, an increase in solvent flow rate from 5.3 to 15.9 $\text{m}^3/(\text{m}^2\cdot\text{h})$ causes an elevation in $K_G a_v$ of as shown in Table 4.5.

Table 4.5 $K_G a_v$ of solvents at each solvent flow rate

$m^3/(m^2 \cdot h)$	$K_G a_v, \text{ kmol}/(\text{kPa} \cdot \text{h} \cdot \text{m}^3)$		
	MEA	2-MAE	DMAE
L=5.3	0.2081	0.3878	0.0103
L=10.6	0.2880	0.5654	0.0137
L=15.9	0.3142	0.6693	0.0139
Slope	0.0100	0.0266	0.0003

From Table 4.5, 2-MAE exhibited the highest slope when solvent concentration was raised from 5.3 to 15.9 $m^3/(m^2 \cdot h)$. According to Section 4.2, bicarbonate formation enhanced CO_2 absorption rate of 2-MAE over MEA and DMAE.

An elevation in solvent flow rate would increase free amine molecules per unit time and let dissolved CO_2 and amine come into contact with each other. Results showed that, though contact time between dissolved CO_2 and amine was reduced due to an increase in solvent flow rate, $K_G a_v$ became larger. Free amine molecules per unit time escalated the rate of reaction to be faster because rate of reaction drastically increased in the early stage as the reactant concentration was still high. This would lead to an increase in enhancement factor. As of Equation (2.14), $K_G a_v$ would raise according to enhancement factor. Besides, wetted surface area which brings gas and liquid into contact would also be higher, leading to transfer of CO_2 in liquid phase.

Figure 4.17 shows that an increase in solvent flow rate leads to a decrease in CO_2 outlet loading. The decline of CO_2 outlet loading implied that CO_2 capture efficiency per mole of amine decreased, though $K_G a_v$ increased, due to shortened in contact time. This should be noted in order to consider whether an increase in solvent flow rate would be necessary or not because solvent circulation rate was reported to be an important parameter, affecting total process cost [22].

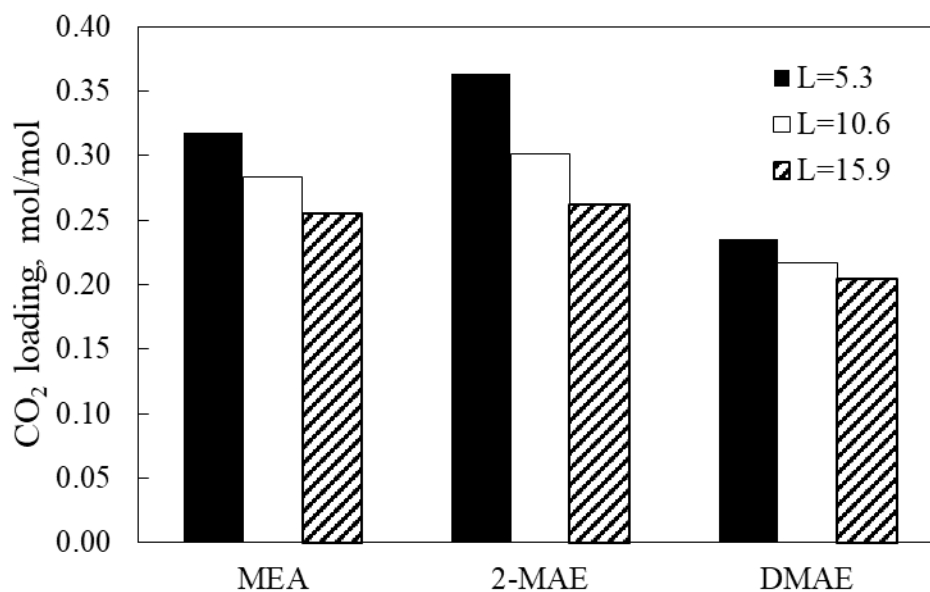


Figure 4.17 CO₂ outlet loading of MEA, 2-MAE and DMAE at solvent flow rate of 5.3, 10.6 and 15.9 m³/(m²·h)

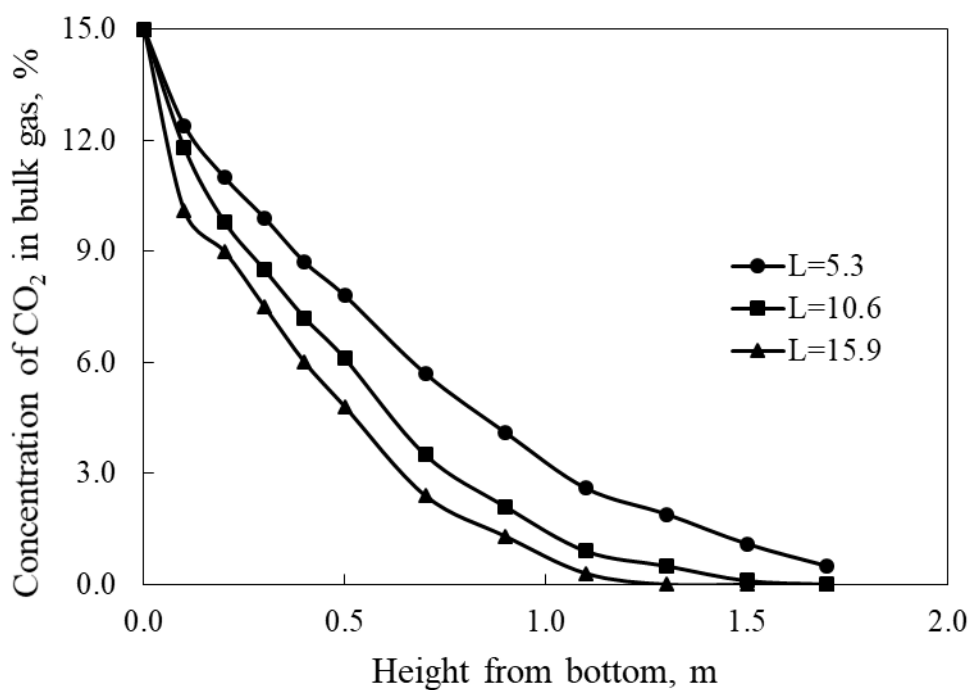


Figure 4.18 CO₂ concentration in bulk gas of MEA against height at solvent flow rate of 5.3, 10.6 and 15.9 m³/(m²·h)

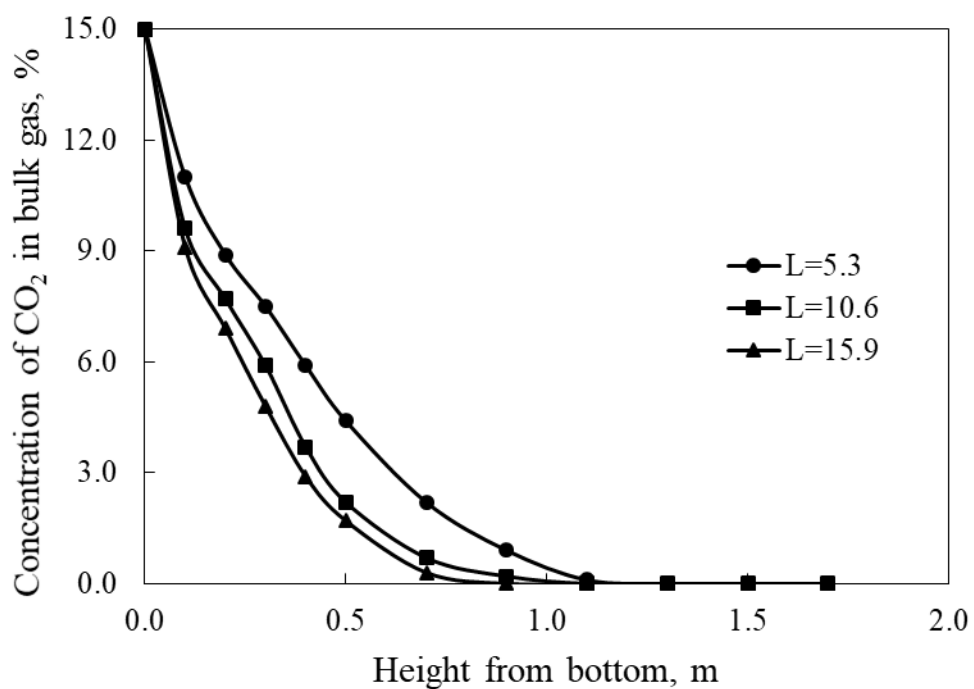


Figure 4.19 CO₂ concentration in bulk gas of 2-MAE against height at solvent flow rate of 5.3, 10.6 and 15.9 m³/(m²·h)

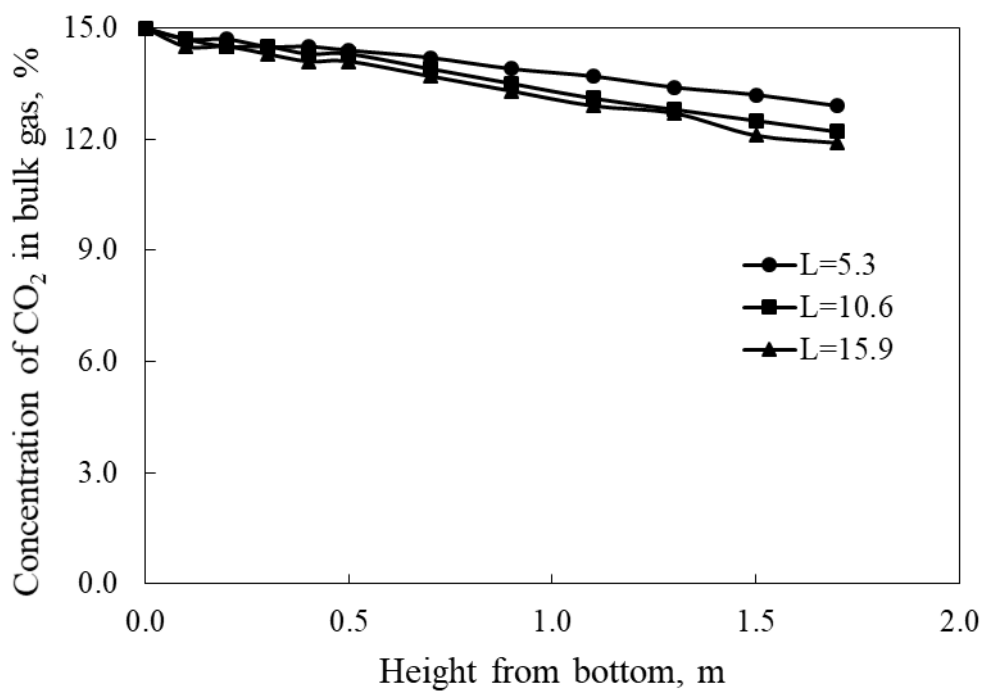


Figure 4.20 CO₂ concentration in bulk gas of DMAE against height at solvent flow rate of 5.3, 10.6 and 15.9 m³/(m²·h)

Figure 4.18, 4.19 and 4.20 reveal that as solvent flow rate increased from $L=5.3$ to $15.9 \text{ m}^3/(\text{m}^2\cdot\text{h})$, $K_G a_v$ also increases, leading to more molecules of CO_2 absorbed along the height of the column. For MEA, at $L=5.3 \text{ m}^3/(\text{m}^2\cdot\text{h})$, only 96.67% of CO_2 removal efficiency was reached at gas outlet while at $L=10.6$ and $15.9 \text{ m}^3/(\text{m}^2\cdot\text{h})$, all CO_2 was absorbed at 1.7 and 1.3 m, respectively.

In case of 2-MAE, at $L=5.3, 10.6$ and $15.9 \text{ m}^3/(\text{m}^2\cdot\text{h})$ CO_2 was depleted at 1.3, 1.1 and 0.9 m, respectively, which implies that the difference between consecutive steps is smaller than that of MEA because of higher rate of reaction. On the other hand, DMAE could not absorb all inlet CO_2 in gas feed. At $L=5.3, 10.6$ and $15.9 \text{ m}^3/(\text{m}^2\cdot\text{h})$, CO_2 absorption efficiency at the exit becomes 14, 18.67 and 20.67%, respectively at the exit. Remaining CO_2 in bulk gas phase directly reflected rate of mass transfer, which showed that DMAE exhibited lowest rate of mass transfer due to its sluggish reaction rate. 2-MAE performed higher rate of mass transfer than MEA and could absorb all CO_2 even in case of $L=5.3 \text{ m}^3/(\text{m}^2\cdot\text{h})$, where MEA could not in the same condition.

จุฬาลงกรณ์มหาวิทยาลัย
CHULALONGKORN UNIVERSITY

4.6 Effect of inert gas flow rate

MEA, 2-MAE and DMAE were examined at the same condition with solvent concentration at 3 kmol/m^3 , CO_2 inlet loading at 0.2 mol/mol , solvent flow rate at $10.6 \text{ m}^3/(\text{m}^2\cdot\text{h})$ and total gas flow rate fixed at 4 L/min in order to compare effect of CO_2 content in feed gas 13-15 v/v% for each solvent type.

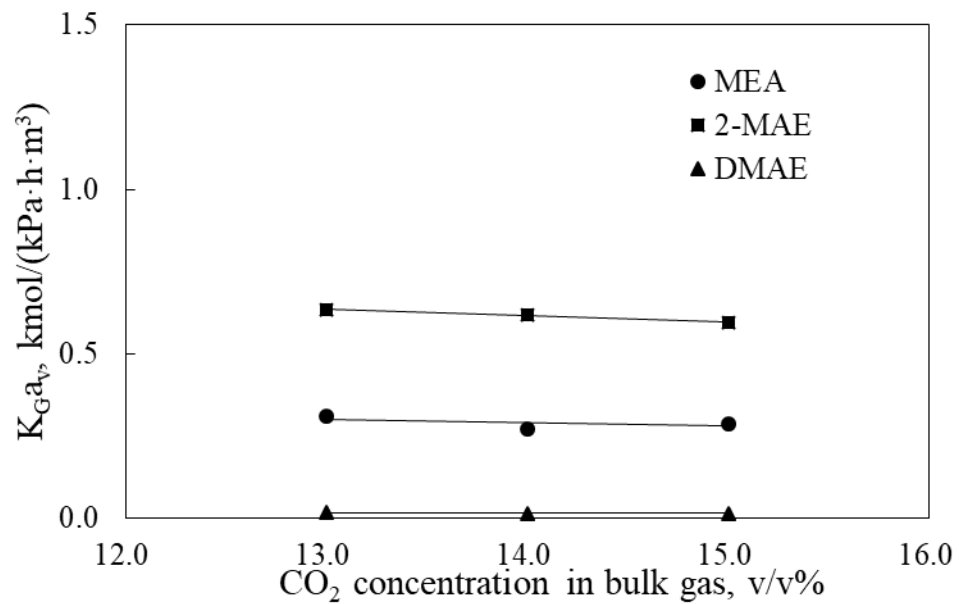


Figure 4.21 Overall mass transfer coefficient of MEA, 2-MAE and DMAE at CO₂ concentration of 13, 14 and 15 v/v%

Figure 4.21 shows that 2-MAE performs the highest mass transfer rate in the investigated range of CO₂ concentration in bulk gas, followed by MEA and DMAE. However, $K_{G a_v}$ of 13-15 v/v% CO₂ content is rather constant for all amines, compared to other factors mentioned before.

Change in CO₂ content in gas phase leads to change in amount of dissolved CO₂ in liquid phase according to Henry's Law. To determine Henry's constant of CO₂-amine systems, N₂O is used instead of CO₂ to detect physical solubility of CO₂ in amine as N₂O does not react with amines and its chemical structure is similar to that of CO₂. From Table 4.6, Henry's constant of CO₂-MEA aqueous system could be calculated from Equation (4.8) [21].

$$H_{\text{CO}_2\text{-MEA}} = H_{\text{N}_2\text{O-MEA}} \left(\frac{H_{\text{CO}_2\text{-H}_2\text{O}}}{H_{\text{N}_2\text{O-H}_2\text{O}}} \right) \quad (4.8)$$

while Henry's constant of CO₂-H₂O and N₂O-H₂O systems could be determined from the same formula in Equation (4.9). Table 4.6 gives constant value of a, b, c and d of each system.

$$H_{\text{CO}_2\text{-H}_2\text{O}}/H_{\text{N}_2\text{O-H}_2\text{O}} = \exp\left(a + \frac{b}{T} + c \ln T + dT\right) \quad (4.9)$$

For N₂O-pure MEA system, Henry's constant could be determined from Equation (4.10) below

$$H_{\text{N}_2\text{O-pure MEA}} = a + bT \quad (4.10)$$

Table 4.6 Henry's constant at 298 K [21]

Solvent system	a	b	c	d	Henry's constant
N ₂ O-H ₂ O	158.245	-9048.596	-20.860	-0.00252	3976.884
CO ₂ -H ₂ O	145.369	-8172.355	-19.303	0	2904.436
N ₂ O-pure MEA	-9172.50	39.598	0	0	2627.704

Penttila et al. reported $H_{\text{N}_2\text{O-MEA}}$ (Henry's constant in N₂O-MEA aqueous system) as a function of solvent composition and temperature of the solvent [21]. With excess properties of solvent applied, calculation of Henry's constant at 298 K yielded $H_{\text{N}_2\text{O-MEA}}=4,325.48$ (kPa·m³)/kmol. According to Equation (4.8), Henry's constant of CO₂-MEA system would be 3159.03 (kPa·m³)/kmol [21]. As equilibrium prevailed at gas-liquid interface, Henry's law could be applied to calculate concentration of CO₂ in liquid phase. Concentration of CO₂ in gas phase according to partial pressure in the

range of 13-15 v/v% CO₂ content could be calculated by Henry's law. From Equation (2.7), Henry's law could be rearranged and written below.

$$y_{\text{CO}_2} P = H c_{\text{CO}_2, i}$$

At $y_{\text{CO}_2}=0.13$, 0.14 and 0.15, CO₂ concentration in liquid phase would be 4.1, 4.5 and 4.8 kmol/m³ at the interface. The study of this effect showed that rate of reaction depended on concentration of amine than CO₂. This could be noticed from effect of CO₂ inlet loading, solvent flow rate and solvent concentration which involved in an increase in concentration or rate of amine feed into the unit volume of absorber.

Variation of CO₂ content in gas phase resulted in little change in CO₂ concentration at gas-liquid interface so rate of reaction was not much different in the range of 13-15 v/v%. Therefore, $K_G a_v$ was only slightly changed over 13-15 v/v%. According to Equation (2.14), three factors affecting overall mass transfer coefficient are k_L^0 , k_g and I as shown below. An increase in CO₂ concentration in bulk gas yielded slight drop in mass transfer coefficient because little drop in inert gas flow rate would lead to thicker gas film. Based on mass transfer with enhancement factor, an increase in CO₂ concentration in bulk gas would lead to nearly equivalent amount of CO₂ solubility in liquid phase (Henry's law) because temperature and pressure of the system were constant. Enhancement factor did not increase as CO₂ concentration in liquid film increased because CO₂ concentration did not affect overall rate of reaction as amine concentration did (see Section 4.3, 4.4 and 4.5)

$$\frac{1}{K_G} = \frac{1}{k_G} + \frac{H}{1k_L^0} \quad (2.14)$$

Comparison between liquid and gas film in the previous section showed that $K_G a_v$ drastically increased when the solvent flow rate increased while it remained quite constant when CO_2 content in bulk gas was raised. An increase in total gas flow rate also not mainly affected the $K_G a_v$ based on packed column similar to this study [18, 19]. This showed that in this study of CO_2 -amine absorption, liquid film was a controlling factor. Figure 4.22 reveals the fact that an elevation of CO_2 concentration in bulk gas would obviously yield higher CO_2 loading capacity at the outlet of the absorber. All three solvents showed the same trend.

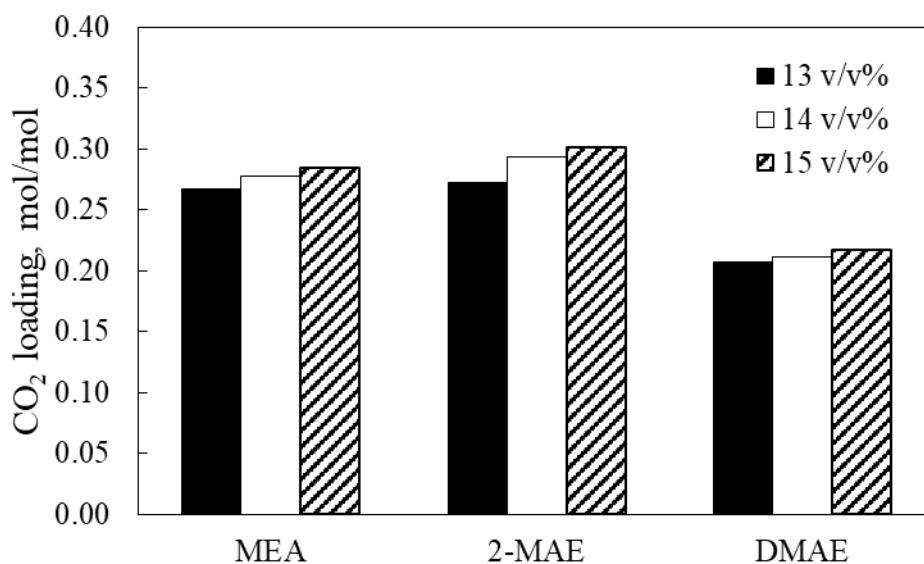


Figure 4.22 CO_2 outlet loading of MEA, 2-MAE and DMAE at CO_2 concentration of 13, 14 and 15 v/v%

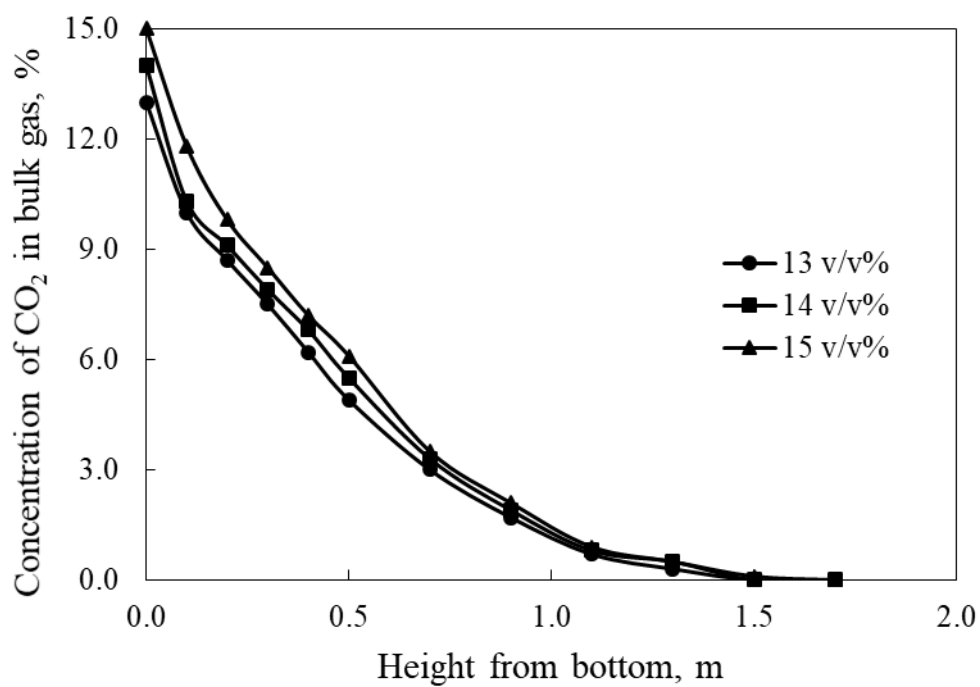


Figure 4.23 CO₂ concentration in bulk gas of MEA against height at CO₂ concentration of 13, 14 and 15 v/v%

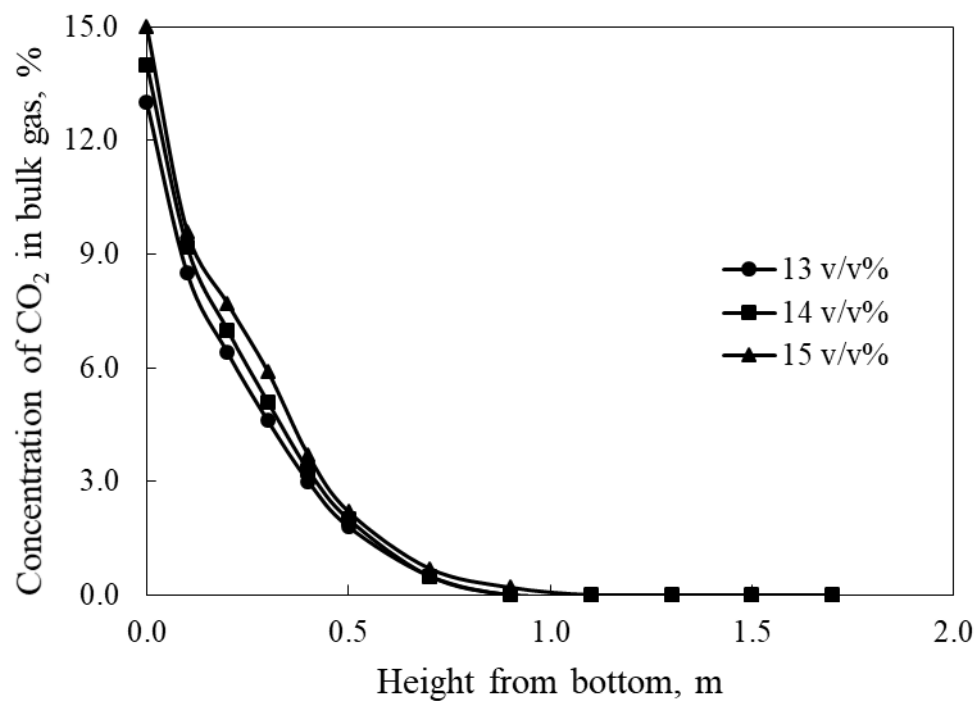


Figure 4.24 CO₂ concentration in bulk gas of 2-MAE against height at CO₂ concentration of 13, 14 and 15 v/v%

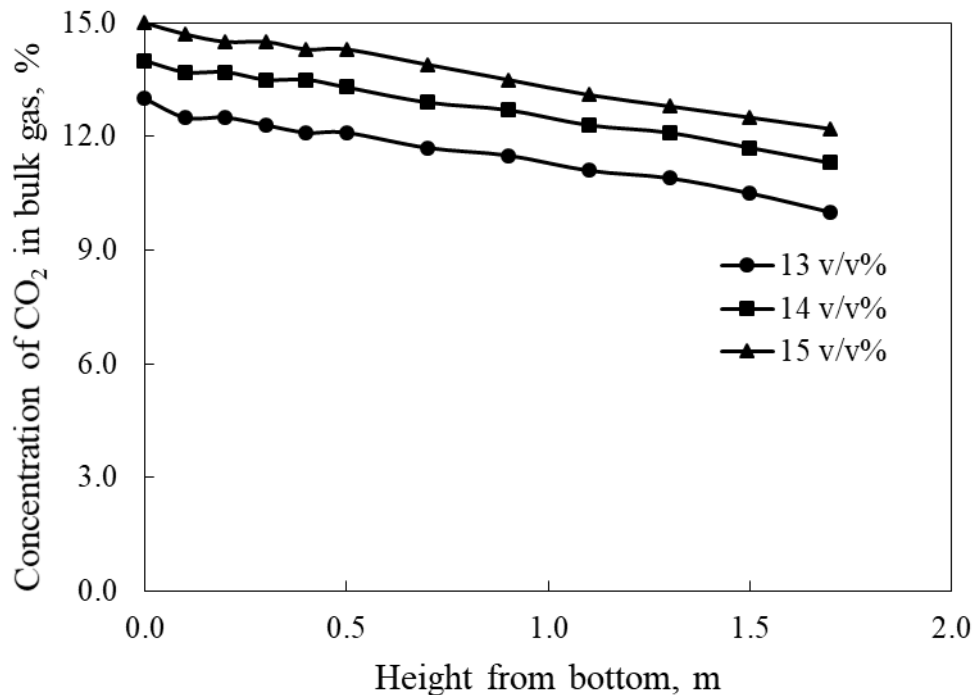


Figure 4.25 CO₂ concentration in bulk gas of DMAE against height at CO₂ concentration of 13, 14 and 15 v/v%

Figure 4.23, 4.24 and 4.25 present that CO₂ concentration in bulk gas decreases along the length of the column. Due to the high CO₂ concentration at the start, 15 v/v% shows the highest CO₂ remaining in bulk gas phase. Nevertheless, all CO₂ concentration (13-15 v/v%) exhibits the same trend for all amines. For MEA, at 13 and 14 v/v%, all CO₂ was absorbed at 1.5 m and, at 15 v/v%, at 1.7 m. In case of 2-MAE, at 13 and 14 v/v%, CO₂ was depleted at 0.9 m and, at 15 v/v%, was at 1.1 m. According to the experimental data, 2-MAE possessed higher K_{Ga_v} than MEA in all cases and therefore required 35.29% less column height than MEA at 15 v/v%. DMAE showed CO₂ removal efficiency of 23.07, 19.29 and 18.67% at CO₂ inlet concentration of 13, 14 and 15 v/v%, respectively. The variation of CO₂ inlet concentration in this case showed that, in the range of coal-fired power plant around 12-18 v/v% [5], K_{Ga_v}

slightly changed. Therefore, little change in CO₂ inlet concentration due to fuel sources would not cause a major problem in CO₂ removal efficiency, but be aware that, in some cases like MEA, if CO₂ inlet concentration was more than 15 v/v%, the CO₂ removal efficiency might not reach 100% at the outlet.



CHAPTER 5

CONCLUSION

5.1 Conclusion

CO₂-MEA, CO₂-2-MAE and CO₂-DMAE absorption systems fell in fast reaction regime because calculated Hatta number was in range of $5I_1 > Ha > \frac{I_1}{5}$ as stated in Section 4.1. According to its characteristics, all dissolved CO₂ reacted with amine within liquid film and consequently no CO₂ left in bulk liquid. However, other reaction products such as carbamate, bicarbonate, and carbonate existed in liquid phase. Enhancement factor of fast reaction regime was inversely proportional to square root of time required for reaction, i.e., time required for amine to absorb CO₂ in liquid film.

2-MAE performed the highest mass transfer rate of 0.5622 kmol/(kPa·h·m³) over MEA which is a conventional amine and DMAE, a tertiary amine. All three solvents possess similar structure of two carbon atoms, a hydroxyl group and an amino group at the other end. 2-MAE and DMAE exhibited one and two methyl groups, respectively, attached to a nitrogen atom. By comparison of solvent types among MEA, 2-MAE and DMAE, 2-MAE showed the highest rate of mass transfer and CO₂ loading capacity due to carbamate instability and bicarbonate formation. Meanwhile, MEA exhibited more carbamate stability so less bicarbonate was formed. DMAE as a tertiary amine could not go through zwitterion route and consequently formed carbonate/bicarbonate instead of carbamate/bicarbonate. Rate of reaction of DMAE was limited by carbonic formation. Therefore, overall rate of mass transfer of DMAE

was the lowest compared to the others. For all conditions, 2-MAE needed the shortest height of absorber followed by MEA and DMAE.

Effect of CO₂ inlet loading capacity at 0.0, 0.1 and 0.2 mol/mol showed that 2-MAE exhibited the highest mass transfer rate of 1.2656 kmol/(kPa·h·m³). As CO₂ inlet loading in absorbent increased, rate of reaction became slower because of lower reactant concentration. Preloaded solvents contained more transformed amine molecules (carbamate, bicarbonate, carbonate, etc.) than unloaded solvents and consequently contained less fresh amine molecules. As reactant concentration increased, time required to absorb CO₂ in liquid film was shortened and consequently enhancement factor increased. Therefore, overall mass transfer coefficient became larger. Moreover, 2-MAE showed a significant drop in mass transfer coefficient when CO₂ inlet loading increased from 0.0 to 0.2 mol/mol while MEA and DMAE did not. This might be a result of too large bicarbonate formation in the solvent. CO₂ outlet loading of 2-MAE was higher than MEA and DMAE representing molecules of absorbed CO₂ throughout the column.

Effect of solvent concentration at 3, 4 and 5 kmol/m³ showed that 2-MAE exhibited the highest mass transfer rate of 0.7211 kmol/(kPa·h·m³). An increase in solvent concentration resulted in more free amine molecules available per unit volume for reaction. Thus, enhancement factor became larger and so was overall mass transfer coefficient. This would be similar to the trend of CO₂ inlet loading. CO₂ outlet loading of 5 kmol/m³ was the smallest compared to 3 and 4 kmol/m³, which showed that, as solvent concentration increased CO₂ capture efficiency per mole of amine decreased.

Effect of solvent flow rate from L=5.3, 10.6 and 15.9 m³/(m²·h) revealed that 2-MAE exhibited the highest mass transfer rate of 0.6693 kmol/(kPa·h·m³) when

$L=15.9 \text{ m}^3/(\text{m}^2\cdot\text{h})$. Higher solvent feed rate resulted in more free amine molecules came into contact with CO_2 in unit volume per unit time. Moreover, wetted surface area between gas and liquid was higher, resulting in higher contact area. With these two factors, rate of mass transfer increased as solvent flow rate increased. CO_2 outlet loading of $L=5.3 \text{ m}^3/(\text{m}^2\cdot\text{h})$ was the highest for all three amines because of longer contact time between CO_2 and amine.

CO_2 content in gas feed 13-15 v/v% showed slight effect on mass transfer rate because of slightly different CO_2 concentration at the interface. Therefore, the controlling factor in this study was the liquid film. Consider effect of CO_2 inlet loading, solvent concentration and solvent flow rate, all of which obviously affected mass transfer coefficient. Amine concentration in solvent played an essential role in CO_2 absorption rate and also mass transfer rate of CO_2 in aqueous amines.

In conclusion, 2-MAE performed the highest mass transfer coefficient of $1.2656 \text{ kmol}/(\text{kPa}\cdot\text{h}\cdot\text{m}^3)$ at solvent concentration of $3 \text{ kmol}/\text{m}^3$, CO_2 inlet loading of $0.0 \text{ mol}/\text{mol}$, CO_2 content of 15 v/v% and solvent flow rate of $5.3 \text{ m}^3/(\text{m}^2\cdot\text{h})$.

In addition, many involved subjects should also be considered when comes to absorbent selection such as energy consumption in solvent regeneration, solvent circulation rate (to meet required treating target), tower sizing, corrosion, etc. In this study, some of the mentioned subjects related to rate of mass transfer were roughly discussed in each section in Chapter4.

5.2 Recommendation

1. Characterization of solvents should be done before and after the experiment to confirm and study the change of each specie.

2. In order to approach industrial process, structured packing would be a good choice to use instead of random packing.



REFERENCES

1. Change, I.P.o.C., *Climate change 2014: mitigation of climate change*. Vol. 3. 2015: Cambridge University Press.
2. Leung, D.Y.C., G. Caramanna, and M.M. Maroto-Valer, *An overview of current status of carbon dioxide capture and storage technologies*. Renewable and Sustainable Energy Reviews, 2014. **39**: p. 426-443.
3. Pongthanaisawan, J. and C. Sorapipatana, *Greenhouse gas emissions from Thailand's transport sector: Trends and mitigation options*. Applied Energy, 2013. **101**: p. 288-298.
4. Wall, T.F., *Combustion processes for carbon capture*. Proceedings of the combustion institute, 2007. **31**(1): p. 31-47.
5. Gupta, M., I. Coyle, and K. Thambimuthu. *CO₂ capture technologies and opportunities in Canada*. in *1st Canadian CC&S Technology Roadmap Workshop*. 2003.
6. Buhre, B.J., et al., *Oxy-fuel combustion technology for coal-fired power generation*. Progress in energy and combustion science, 2005. **31**(4): p. 283-307.
7. Yu, C.-H., C.-H. Huang, and C.-S. Tan, *A review of CO₂ capture by absorption and adsorption*. Aerosol Air Qual. Res, 2012. **12**(5): p. 745-769.
8. Li, X., S. Wang, and C. Chen, *Experimental study of energy requirement of CO₂ desorption from rich solvent*. Energy Procedia, 2013. **37**: p. 1836-1843.
9. Chakravarti, S., A. Gupta, and B. Hunek. *Advanced technology for the capture of carbon dioxide from flue gases*. in *First National Conference on Carbon Sequestration, Washington, DC*. 2001. Citeseer.
10. Wang, M., et al., *Post-combustion CO₂ capture with chemical absorption: A state-of-the-art review*. Chemical Engineering Research and Design, 2011. **89**(9): p. 1609-1624.
11. Nielsen, C.J., H. Herrmann, and C. Weller, *Atmospheric chemistry and environmental impact of the use of amines in carbon capture and storage (CCS)*. Chemical Society Reviews, 2012. **41**(19): p. 6684-6704.
12. Boot-Handford, M.E., et al., *Carbon capture and storage update*. Energy & Environmental Science, 2014. **7**(1): p. 130-189.
13. Li, L. and G. Rochelle, *CO₂ mass transfer and solubility in aqueous primary and secondary amine*. Energy Procedia, 2014. **63**: p. 1487-1496.
14. Kohl, A.L. and R. Nielsen, *Gas purification*. 1997: Gulf Professional Publishing.
15. Vaidya, P.D. and E.Y. Kenig, *CO₂-Alkanolamine reaction kinetics: A review of recent studies*. Chemical Engineering & Technology, 2007. **30**(11): p. 1467-1474.
16. Aroonwilas, A., A. Veawab, and P. Tontiwachwuthikul, *Behavior of the mass-transfer coefficient of structured packings in CO₂ absorbers with chemical reactions*. Industrial & engineering chemistry research, 1999. **38**(5): p. 2044-2050.
17. Maneeintr, K., et al., *Comparative mass transfer performance studies of CO₂ absorption into aqueous solutions of DEAB and MEA*. Industrial & Engineering Chemistry Research, 2010. **49**(6): p. 2857-2863.

18. Wen, L., et al., *Comparison of Overall Gas-Phase Mass Transfer Coefficient for CO₂ Absorption between Tertiary Amines in a Randomly Packed Column*. Chemical Engineering & Technology, 2015. **38**(8): p. 1435-1443.
19. Sema, T., et al., *Comprehensive mass transfer and reaction kinetics studies of a novel reactive 4-diethylamino-2-butanol solvent for capturing CO₂*. Chemical Engineering Science, 2013. **100**: p. 183-194.
20. Zhang, W., et al., *Parametric study on the regeneration heat requirement of an amine-based solid adsorbent process for post-combustion carbon capture*. Applied Energy, 2016. **168**: p. 394-405.
21. Penttilä, A., et al., *The Henry's law constant of N₂O and CO₂ in aqueous binary and ternary amine solutions (MEA, DEA, DIPA, MDEA, and AMP)*. Fluid Phase Equilibria, 2011. **311**: p. 59-66.
22. Astaria, G., D. W. Savage, and A. L. Bisio, *Gas Treating With Chemical Solvents*. 1983.
23. Aronu, U.E., et al., *Solubility of CO₂ in 15, 30, 45 and 60 mass% MEA from 40 to 120 C and model representation using the extended UNIQUAC framework*. Chemical Engineering Science, 2011. **66**(24): p. 6393-6406.
24. Haider, H.A., R. Yusoff, and M. Aroua, *Equilibrium solubility of carbon dioxide in 2 (methylamino) ethanol*. Fluid Phase Equilibria, 2011. **303**(2): p. 162-167.
25. Welty, J.R., et al., *Fundamentals of momentum, heat, and mass transfer*. 2009: John Wiley & Sons.
26. Zeng, Q., et al., *Mass transfer coefficients for CO₂ absorption into aqueous ammonia solution using a packed column*. Industrial & Engineering Chemistry Research, 2011. **50**(17): p. 10168-10175.
27. Naami, A., et al., *Analysis and predictive correlation of mass transfer coefficient KGav of blended MDEA-MEA for use in post-combustion CO₂ capture*. International Journal of Greenhouse Gas Control, 2013. **19**: p. 3-12.
28. Levenspiel, O., *Chemical reaction engineering*. Industrial & engineering chemistry research, 1999. **38**(11): p. 4140-4143.
29. Snijder, E.D., et al., *Diffusion coefficients of several aqueous alkanolamine solutions*. Journal of Chemical and Engineering data, 1993. **38**(3): p. 475-480.
30. Kortunov, P.V., et al., *In situ nuclear magnetic resonance mechanistic studies of carbon dioxide reactions with liquid amines in aqueous systems: New insights on carbon capture reaction pathways*. Energy & Fuels, 2015. **29**(9): p. 5919-5939.
31. Satesh, G., M.A.T. M., and Z. Han, *Carbamate Stabilities of Sterically Hindered Amines from Quantum Chemical Methods: Relevance for CO₂ Capture*. ChemPhysChem, 2013. **14**(17): p. 3936-3943.
32. van de Haar, A., et al., *Dynamics of Postcombustion CO₂ Capture Plants: Modeling, Validation, and Case Study*. Industrial & Engineering Chemistry Research, 2017. **56**(7): p. 1810-1822.
33. Artanto, Y., et al., *Pilot-scale evaluation of AMP/PZ to capture CO₂ from flue gas of an Australian brown coal-fired power station*. International journal of Greenhouse Gas control, 2014. **20**: p. 189-195.

34. McCann, N., M. Maeder, and H. Hasse, *Prediction of the overall enthalpy of CO₂ absorption in aqueous amine systems from experimentally determined reaction enthalpies*. Energy Procedia, 2011. **4**: p. 1542-1549.



APPENDIX

Appendix A.1 Nomenclature

Symbol	Definition	Unit
a_v	Interfacial area between gas and liquid phase per unit volume of absorber	$\frac{\text{m}^2}{\text{m}^3}$
D	Diffusivity coefficient	$\frac{\text{m}^2}{\text{s}}$
$c_{\text{CO}_2,i}$	Concentration of CO_2 at gas-liquid interface	$\frac{\text{kmol}}{\text{m}^3}$
$c_{\text{CO}_2,l}$	Concentration of CO_2 in bulk liquid phase	$\frac{\text{kmol}}{\text{m}^3}$
G_{CO_2}	Molar flow rate of CO_2 per cross-sectional area per hour	$\frac{\text{kmol}}{\text{m}^2 \cdot \text{h}}$
G_I	Molar flow rate of inert gas per cross-section area per hour	$\frac{\text{kmol}}{\text{m}^2 \cdot \text{h}}$
H	Henry's constant	$\frac{\text{kmol}}{\text{m}^3 \cdot \text{kPa}}$
Ha	Hatta Number	-
I	Enhancement factor	-
k	rate constant	$\frac{\text{m}^3}{\text{kmol} \cdot \text{s}}$
k_G	Gas side mass transfer coefficient	$\frac{\text{kmol}}{\text{m}^2 \cdot \text{h}} \cdot \frac{\text{m}^3}{\text{kmol}}$
K_G	Overall mass transfer coefficient based on gas phase	$\frac{\text{kmol}}{\text{kPa} \cdot \text{h} \cdot \text{m}^2}$
k_L^0	Liquid side mass transfer coefficient without chemical reaction	$\frac{\text{kmol}}{\text{m}^2 \cdot \text{h}} \cdot \frac{\text{m}^3}{\text{kmol}}$
k_L	Liquid side mass transfer coefficient with chemical reaction	$\frac{\text{kmol}}{\text{m}^2 \cdot \text{h}} \cdot \frac{\text{m}^3}{\text{kmol}}$
$K_G a_v$	Volumetric overall mass transfer coefficient	$\frac{\text{kmol}}{\text{m}^3 \cdot \text{kPa} \cdot \text{h}}$
N_{CO_2}	Molar flux of CO_2 transferring from gas to liquid	$\frac{\text{kmol}}{\text{m}^2 \cdot \text{h}}$
P	Total pressure of the system	kPa

Symbol	Definition	Unit
$p_{\text{CO}_2,g}$	Partial pressure of CO ₂ in bulk gas phase	kPa
$p_{\text{CO}_2,i}$	Partial pressure of CO ₂ at gas-liquid interface	kPa
$p_{\text{CO}_2}^*$	Partial pressure of CO ₂ that in equilibrium with $c_{\text{CO}_2,l}$	kPa
x	Distance that CO ₂ molecules travel into liquid film	m
$y_{\text{CO}_2,g}$	Mole fraction of CO ₂ in bulk gas phase	-
$y_{\text{CO}_2}^*$	Mole fraction of CO ₂ that equilibrium with $c_{\text{CO}_2,l}$	-

Appendix A.2 Abbreviation

2-MAE = 2-(Methylamino)ethanol

DMAE = Dimethylaminoethanol

MEA = Monoethanolamine

Appendix B Overall CO₂ mole balance

In case of MEA concentration at 3 kmol/m³, CO₂ inlet loading at 0.0 mol/mol, solvent flow rate at 10.6 m³/(m²·h) or 0.080 L/min, CO₂ content at 15 v/v%.

CO₂ Inlet

CO₂ inlet (mol/min) could be determined from mass flow meter according to Ideal gas law where $P=1.01 \times 10^2$ kPa, $\dot{V}=0.60$ L/min, $R=8.314$ L · kPa · K⁻¹mol⁻¹, $T=298$ K

$$P\dot{V} = nRT$$

$$\dot{n} = \frac{(1.01 \times 10^2)(0.60)}{(8.314)(298)}$$

$$\dot{n} = 0.0245 \text{ mol/min}$$

CO₂ Outlet

CO₂ outlet (mol/min) could be determined from CO₂ outlet loading measured by titration with HCl as described in Section 3.2.2.

$$\text{CO}_2 \text{ outlet loading} = 0.100 \text{ mol CO}_2/\text{mol MEA}$$

$$\text{Average solvent outlet flow rate} = 7.889 \times 10^{-2} \text{ L/min}$$

$$\text{CO}_2 \text{ outlet } \left(\frac{\text{mol}}{\text{min}} \right) = \frac{0.1 \text{ mol CO}_2}{\text{mol MEA}} \times \frac{7.889 \times 10^{-2} \text{ L}}{\text{min}} \times \frac{3 \text{ mol MEA}}{\text{L}}$$

$$\text{CO}_2 \text{ outlet } \left(\frac{\text{mol}}{\text{min}} \right) = 0.0237 \text{ mol/min}$$

Difference of CO₂ inlet and outlet mole per minute could be calculated from

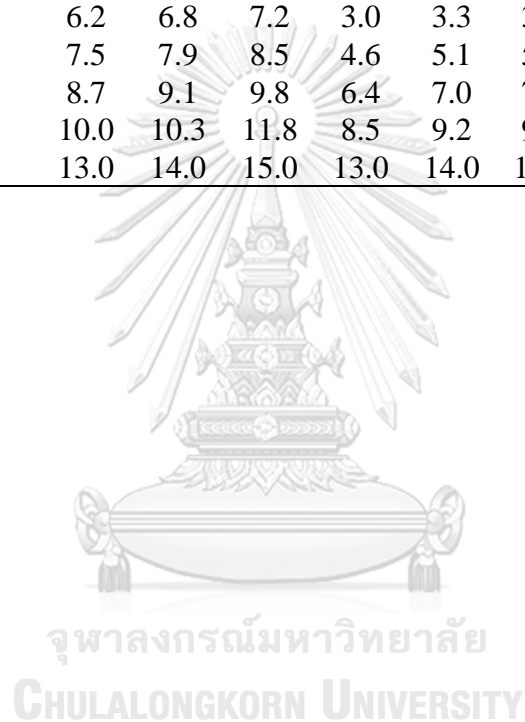
$$\text{Error (\%)} = \frac{0.0245 - 0.0237}{0.0237} \times 100 = 3.38\%$$

Error of 3.38% is tolerable because, in this field of study, upto 10% is acceptable.



Appendix C.5 CO₂ content in bulk gas (v/v%) in each of inert gas flow rate

Height from bottom, m	MEA			2-MAE			DMAE		
	13	14	15	13	14	15	13	14	15
1.7	0.0	0.0	0.0	0.0	0.0	0.0	10.0	11.3	12.2
1.5	0.0	0.0	0.1	0.0	0.0	0.0	10.5	11.7	12.5
1.3	0.3	0.5	0.5	0.0	0.0	0.0	10.9	12.1	12.8
1.1	0.7	0.8	0.9	0.0	0.0	0.0	11.1	12.3	13.1
0.9	1.7	1.9	2.1	0.0	0.0	0.2	11.5	12.7	13.5
0.7	3.0	3.3	3.5	0.5	0.5	0.7	11.7	12.9	13.9
0.5	4.9	5.5	6.1	1.8	2.0	2.2	12.1	13.3	14.3
0.4	6.2	6.8	7.2	3.0	3.3	3.7	12.1	13.5	14.3
0.3	7.5	7.9	8.5	4.6	5.1	5.9	12.3	13.5	14.5
0.2	8.7	9.1	9.8	6.4	7.0	7.7	12.5	13.7	14.5
0.1	10.0	10.3	11.8	8.5	9.2	9.6	12.5	13.7	14.7
0.0	13.0	14.0	15.0	13.0	14.0	15.0	13.0	14.0	15.0



VITA

Parintorn Vaewhongs was born on May the 1st in 1993. She graduated high school course from Sacred Heart Convent School in 2011. In 2016, she earned Bachelor Degree in Chemical Engineering, Faculty of Engineer, Kasetsart University.

